Advanced Power Sharing Scheme under Unbalanced and Nonlinear Loads in an Islanding Microgrid

A Thesis

Presented to

The Faculty of the Department of Electrical and Computer Engineering

University of Houston

In Partial Fulfillment

Of the Requirements for the Degree

Masters of Science

In Electrical Engineering

By

Mehmet Emin Akdogan

August 2017

Advanced Power Sharing Scheme under Unbalanced and Nonlinear Loads in an Islanding Microgrid

Mehmet Emin Akdogan

Approved:

Chair of the Committee
Dr. Mehdi Abolhassani, Assistant Professor,
Electrical and Computer Engineering,
Electrical Engineering Technology

Committee Members:

Dr. Kaushik Rajashekara, Professor,
Electrical and Computer Engineering

Dr. David P. Shattuck, Associate Professor,
Electrical and Computer Engineering

Dr. Suresh K. Khator, Associate Dean,
Cullen College of Engineering

Dr. Badri Roysam, Professor and Chair,
Electrical and Computer Engineering

ACKNOWLEDGEMENT

Foremost, I would like to express my sincere gratitude to my advisor, Dr. Mehdi Abolhassani, for the continuous support of Master's study and research, for his patience, motivation, enthusiasm, and immense knowledge. This guidance helped me a lot to finish my research and writing of this thesis. I could not have imagined a better advisor and mentor for my Master's study.

Besides my advisor, I would like to thank the rest of my thesis committee, Dr. Kaushik Rajashekara and Dr. David P. Shattuck, for their encouragement, insightful comments, and positive feedback.

I would also like to show my appreciation to the department of Electrical and Computer Engineering for giving me the opportunity to be a part of well-organized program and provide me with resources to complete my research.

I thank my fellow lab mates at University of Houston for the stimulating discussions, for the sleepless nights we were working together before the deadlines, and for all the fun we had in the last two years. In addition, I would like to thank my roommate, Ahmet Emirhan Yolcu, for driving and supporting me during the thesis work.

Last but not the least, I would like to use this opportunity to thank my parents, Atiye Akdogan and Kasim Akdogan, and my sisters and brother for the priceless foundation they laid many years ago. None of these accomplishments would have been possible without their sacrifices. They are the best parents anyone could have wished for and I dedicate this thesis to them.

Advanced Power Sharing Scheme under Unbalanced and Nonlinear Loads in an Islanding Microgrid

An Abstract

of a

Thesis

Presented to

The Faculty of the Department of Electrical and Computer Engineering

University of Houston

In Partial Fulfillment

Of the Requirements for the Degree

Masters of Science

In Electrical Engineering

By

Mehmet Emin Akdogan

August 2017

ABSTRACT

Active, unbalanced, and harmonic power sharing inaccurately between distributed generators (DGs) and voltage quality problems are critical issues under unbalanced and nonlinear loads in the micro grids. Thus, an advanced power sharing scheme with unbalanced and harmonic loads in islanding micro grid is presented to eradicate power sharing problems and reduce unbalanced voltage and harmonics distortion. The hierarchical control structure comprises primary and secondary levels. For improving voltage quality, a secondary controller is designed to manage compensation of unbalanced and harmonic voltage at point common coupling (PCC). The Primary controller consists of distributed generators local controllers. The local controllers mainly include power droop for sharing active and reactive power among DGs without communication, voltage and current controllers, and virtual impedance control loop. Virtual impedance loop for positive and negative sequences of fundamental and harmonic components is used to achieve better power sharing of reactive, unbalance and harmonic powers. The design procedure of the hierarchical control structure is discussed in detail.

The proposed approach is able to operate in islanded micro grids for voltage quality enhancement. Effectiveness of the hierarchical power sharing scheme is presented on MATLAB/Simulation and the simulation results of the proposed method are provided to demonstrate that PCC voltage distortion decreased from 9.47% to 4.62% while reactive, unbalanced, and harmonic powers is shared proportionally among DGs after compensation.

TABLE OF CONTENTS

LIST OF FIGURES

LIST OF TABLES

ACRONYMS

VSI	Voltage source inverter
MG	Microgrid
RES	Renewable energy resource.
ESS	Energy storage systems
APF	Active power filter
SRF	Synchronous reference frame
PCC	Point of common coupling
PV	Photovoltaics
DG	Distributed generator
PWM	Pulse Width Modulator
SOGI	Second order generalized integrator
LCL	Inductor-capacitor-inductor
THD	Total harmonic distortion
VUF	Voltage unbalanced factor
FPS	Fundamental positive-sequence
VPI	Virtual positive-sequence impedance.
VPI	Virtual negative-sequence impedance
VVHI	Virtual variable harmonic impedance.
PR	Proportional resonant
VSC	Voltage source converter
PI	Proportional integral.

PLL	The phase locked loop
$\boldsymbol{P}^{+}$,$\boldsymbol{Q}^{+}$	Positive-sequence real and reactive powers at fundamental frequency.
SOC	Switch
LPF	Low pass filter.
BPF	Band pass filter

CHAPTER 1 INTRODUCTION

The electrical grid becomes a more decentralized and intelligent network along with the fast technology progress in distributed generation (DG), while environmental concern and the energy security are growing [34]. Instead of a traditional grid, the new electrical grid, also named as smart grid, is the collection of all technologies, concepts and approaches for improved efficiency, reliability and safety, with smooth integration of renewable and alternative energy sources to allow hierarchies of generation, transmission, and distribution through distributed automated energy delivery network technologies [1-5].

A smart grid, using two-way flows of electricity and information, is also a self-healing system to predict looming failures and takes corrective action to avoid or mitigate system problems [1-2]. In a smart grid, the consumers are able to interact with an energy management system in order to adjust the energy consumption and reduce the energy cost [6]. Some attractive advantages of the smart grid are as follow:

- Improving power reliability and quality
- Enhancing capacity and efficiency of existing electric power networks
- Facilitating expanded deployment of renewable energy sources
- Accommodating distributed power sources
- Automating maintenance and operation
- Improving grid security [2].

While electrical grid is transformed to decentralized system, several challenges exists on the architecture of power systems. Therefore as the main block of a smart grid and an effective complement to large power grid, Micro grid (MG) concept, has been widely developed as an attractive solution for the architectures of future grids.

Although conventional grids generate, distribute and regulate the flow of electricity to consumers centrally, as the main block of smart grid, micro grids consisting of distributed generations, energy storage systems and dispersed load can become completely independent from the main grid and operate locally. Micro grid is a local grid to integrate multiple DG units to reduce the impact of high DG penetration on power system operation and improve the service reliability [7] [9]. Advantages of micro grid are increasing power quality, reliability and controllable. It can operate both in main grid connected (utility grid) mode and autonomous islanding mode. Unlike traditional grids, a micro grid can switch to autonomous islanding operation during main grid faults and DG interfacing converters can obtain a direct voltage support [7-11].

When renewable energy such as wind turbines, photovoltaic panels and fuel cells is available, distributed generation has been widely used in recent years, because of growing demand for electricity and attention environmental protection and increasing penetration of renewable energy sources. Distributed generation like wind generation, photovoltaic (PV) generation, fuel cell generation, energy storage systems (ESS) is connected to MGs through power electronics interface converter such as inverters or ac-ac converters to make up local ac grids [7], [8],[11]. DGs interface converter, a voltage source inverter in islanded operation, is connected to an AC common bus to share properly the disperse loads connected to the local grid. In addition, DG interface inverters in micro grids set output voltage amplitude and phase angle to inject the active and reactive powers and to produce highly reliable and good quality electrical power [35]. Furthermore, inductor-capacitor-inductor (LCL) filters are usually used as an interface between the inverter and the local loads is integrated to attenuate the switching frequency current harmonics.

1.1 Problem Definitions and Existing Solutions

To avoid circulating currents among the DG units and ensure stable and efficient operation, MGs form some controls [37]. In addition, every DG unit should operate independently and in parallel also without communication due to long distance between DGs. However, increasing of penetration of DG systems may bring problems like inverse power flow, voltage deviation, and voltage fluctuation to the distribution networks [10]. Therefore, it should be noted that some proper micro grid control methods are adopted to DG interface inverters to regulate power quality problems to reduce harmonic distortion and to achieve better operation of multiple parallel DGs units [6], [9] and [13]. Also, the method is designed to manage active and reactive power control capabilities among the DGs, energy management, frequency and voltage regulation, and economic optimization [37].

One of the micro grid controls which is droop control has been designed because each DG unit should be controlled to be proportional to its power rating in the islanded mode [10]. Thus, to share active and reactive power without communication between DGs and improve reliability of micro grid islanded grid modes, some droop control has been presented in [6] [8] [9] [10]. On the other hand, lack of conventional droop control is compromising of power sharing accuracy and voltage distortion. In addition, conventional droop control does not share active power proportionally [12]. To overcome those problems, active and reactive power control has been adopted. However, sharing of reactive power properly, harmonic current sharing have still drawbacks thus, virtual impedance is proposed to improve sharing powers better among DGs and to enhance the reliability and performance of the droop-controlled, for ensuring the inductive behavior of the output impedance of the DGs. As a result, the droop control has been widely used in microgrid applications with virtual impedance loops, which ensures some impedance between voltage sources. This way, the current flow between inverters is reduced and output impedance magnitude and phase angle can be fixed [36].

Unbalanced loads in three phase micro grid may be adopted. A major cause of voltage unbalance is the connection of unbalanced loads. Unbalanced load means single-phase loads are connected between two phases or between one phase and the neutral. It causes unbalance voltage, negative sequence of voltage fundamental component. Definition of unbalanced voltage is that any difference exists in the three phase voltage magnitudes and/or a shift in the phase separation from 120 degrees and otherwise the voltage is unbalanced [38].

To simplify analysis of power systems under unbalanced conditions, symmetrical components theory is used to decompose a three-phase unbalanced voltage into three symmetrical sets of balanced sequences, namely the positive, negative, and zero-sequence components. It should be noted that the sum of those three sets are three-phase unbalanced voltage in Fig 1.1, positive sequence has equal magnitude and ±120° phase displacement in counter clockwise direction, negative sequence contains the same magnitude and but the direction of rotation is opposite of the positive sequence phasors (rotated 120° in clockwise direction) [39]. In addition, rotation does not exist between zero sequence components. Note that, negative sequence and zero sequence components does not exists, if the voltage is perfectly balanced.

The relationship between three-phase unbalanced voltage phasor and symmetrical components can be written as

$$\begin{bmatrix} V_A \\ V_B \\ V_C \end{bmatrix} = \begin{bmatrix} 1 & 1 & 1 \\ 1 & a^2 & a \\ 1 & a & a^2 \end{bmatrix} . \begin{bmatrix} V^+ \\ V^- \\ V^0 \end{bmatrix} \text{ and}$$

(1.1)

$$\begin{bmatrix} V^+ \\ V^- \\ V^0 \end{bmatrix} = \begin{bmatrix} 1 & 1 & 1 \\ 1 & a^2 & a \\ 1 & a & a^2 \end{bmatrix} . \begin{bmatrix} V_A \\ V_B \\ V_C \end{bmatrix}, \qquad (1.2)$$

where V_A, V_B and V_C are the voltage phasors; V^+, V^- and V^0 are the positive, negative and zero symmetrical systems, respectively; a = j 120 is the rotation operator.

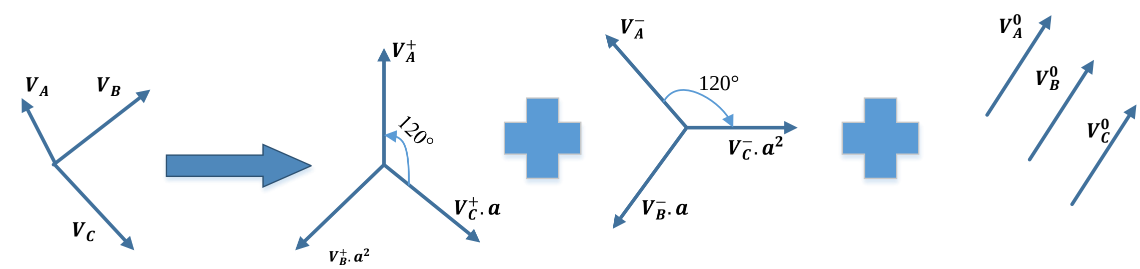

Fig 1.1. Decomposition of an Unsymmetrical Phasors System in Three Symmetrical Phasor Systems

The synchronous or asynchronous generators create positive sequence components, while the negative and zero sequence components appear at the place of unbalance. Each of the sequences can be separately measured and influences in a different way in the power system [39]. However, voltage unbalance is power quality problem on power systems and equipment. These problems are over voltage, overheating, vibration and intermittent shutdown on electrical equipment such as induction motors, power electronic converters. Moreover under unbalanced conditions, power losses on the system will increase and the system may be unstable. Hence, the International Electro technical Commission (IEC) recommends the limit of 2% for voltage unbalance in electrical systems [16], [6]. To overcome unbalanced power problems, unbalance compensation approach in [24] is proposed. Voltage unbalanced is compensated using shunt active power. Moreover negative sequence current is injected by DG for compensation unbalanced voltage in [18].

Different nonlinear loads such as rectifiers load might be also connected in distributed generations. Nonlinear loads create voltage harmonic distortion, positive and negative sequence of voltage main harmonics. However, they are able to cause deterioration of power quality and voltage distortions and harmonic propagation along a distribution feeder. These issues are protective relays malfunction, overheating of motors and transformers and failure of power factor correction capacitors. The micro grid becomes much weaker and more sensitive to harmonic disturbances. Hence, the reduction of harmonic voltage distortions is important under nonlinear load conditions for stable operation of micro grids. Thus, Based on the IEEE standard 519-1992 [19], the voltage Total harmonic distortion (THD) for sensitive loads should be maintained below 5%. To cope harmonic distortion problems, some harmonics compensation methods have been presented in [6], [14-15]. DG unit imitates a resistance at harmonic frequency and supply a harmonic power droop in order to share compensation effort between DGs.

The method presented in [11] is based on using active power filter (APF) to compensate voltage unbalance harmonic by injecting negative sequences to distribution line. However it is uneconomic to install extra APF for each DGs in islanded micro grids. Moreover, voltage source inverters that control and transfer power can control unbalance voltage compensation properly [10], [6]. Moreover, it should be noted that the unbalanced harmonic compensation methods are proposed to enhance unbalance harmonics voltage at the DG terminal while the voltage quality at the point of common coupling should be considered for sensitive loads [20].

Active, reactive, unbalance and harmonic power sharing inaccurately between DGs and voltage quality problems are important affair under unbalance and nonlinear loads in the micro grids. Thus positive and negative sequences of fundamental and main harmonic voltage should be compensated in secondary control. While droop control is considered for active and reactive power sharing accurately, Virtual impedance will be implemented for unbalanced harmonic power sharing issue. Finally, the test system will be simulated on MATLAB simulator.

1.2 Literature Review

Some work has been proposed for power sharing problems and to reduce unbalanced voltage and harmonics distortion as follow in [6]-[9-11].

Voltage unbalance and harmonic compensation method in [11] has presented using PI plus multi resonant controller to improve voltage quality in a single fundamental positive-sequence (FPS) synchronous reference frame (SRF) for islanded micro grid. Proposed control consists of power droop controller and modified virtual impedance. Conventional PI controller only regulates DC component which is fundamental positive sequence (FPS). So it is unsatisfied to reduce unbalance harmonic distortion. PI plus multi resonant is adopted to compensate AC components. However the harmonic voltage drop exist across the total output impedance therefore modified virtual impedance by inserting LPF to reduce harmonic components. Simulation in MATLAB and experimental prototype on a RT-LAB environment result approved effectiveness of proposed control strategy under unbalance and diode bridge rectifier loads. On the other hand, a proportional integral (PI) plus multi-resonant voltage controller is proposed only in a single fundamental positive-sequence (FPS). With proposed method, voltage distortion by fundamental negative sequence and selective main harmonic sequence could not be eliminated for sensitive loads.

Secondary control for compensating unbalance voltage to adjust voltage of PCC and frequency level in islanded micro grid has been presented in [6]. Secondary controller is designed to manage compensation of unbalance voltage at PCC and restore voltage and frequency by sending proper control signals to the primary level. Closed loop transfer function G(s) and output impedance (Zo) of control system has been discussed and a voltage reference is insured for negative and positive sequences at primary control. Moreover, stability of unbalance compensation system is also provided by proposing small signal analysis method. Simulation results demonstrate that voltage unbalance factor improved voltage quality of PCC while negative sequence voltage is decreased. However, the method just proposed secondary control for unbalance conditions, there is no nonlinear load for harmonics and no compensation effort to produce reference voltage. In addition, fundamental negative sequence of load current are avoided for sharing properly base on drop control and virtual impedance during the unbalance conditions.

The approach presented in [9] is based on applying secondary control to improve SLB unbalance and harmonic voltage quality by sending proper control signal to DGs in the hierarchical control. As a new method, if DGs have different rated power, compensation control effort for sharing proportionally compensation effort between DGs also is proposed in the paper. DG local control is implemented in αβ frame and LBC is extracted in dq frame. The effeteness of the proposed control scheme in simulation results is validated that SLB voltage distortion decreased noticeably while load current sharing is improved properly after compensation. However, unbalance harmonic compensation (UHC) is not adopted to reduce unbalance harmonic voltage to provide better voltage quality.

In [10], power sharing enhancement control method has been proposed to reduce unequal current sharing error and to compensate reactive, unbalance and harmonic power sharing problems under unbalanced and nonlinear load in the islanded ac micro grid. In primary control, DSC-SOGI (delayed signal cancellation with secondary order organization integrator) base sequence decomposition is presented to extracts the fundamental positive/negative and harmonic current components for virtual impedance loop. In addition, new proposed method, unbalance and harmonic compensation method, producing a reference, is adopted to decrease unbalance (negative sequence) and harmonic power sharing problems. Auxiliary control which consists compensation effort control managing selective main harmonic compensation of PCC voltage to share among DG units. However, unbalance (fundamental negative sequence) of current is not extracted to calculate unbalanced factor and generated compensation reference of fundamental negative sequence in compensation effort controller. In addition the lack of proposed method is that DG units is equal capacities so powers may not be shared properly if DG units have different rated power in the paper.

CHAPTER 2 PROPOSED HIERARCHICAL CONTROL IN MICROGRID

In a typical micro grid system, proposed hierarchical control structure which is connected to power stage of a DG unit is demonstrated in Fig 2.1. The proposed control contains two levels. DG local control is primary control to share power in this level. Secondary control is for PCC voltage quality improvement. It should be noted that after PCC voltage compensation in secondary control, output of secondary control sends the data to all DGs to improve PCC voltage. The power stage of each DG unit includes an interface inverter and LC filter and a dc link. It is assumed that an approximately constant dc link voltage (Vdc) is maintained at the dc link. In addition, a feedforward loop is included in order to take the small variations of dc link voltage (Vdc) in generation of the inverter gate signals by pulse width modulator (PWM). For facilitation, power stage of DG1 and connection line DG1 are shown in Fig 2.1. Note that there might be more than one DG connected power stages. There are two voltage and current measurement points as DG terminal and PCC where DG terminal is output of filter and PCC is integrated point of loads (linear, unbalanced and nonlinear loads). For each DG unit, dc power (v_{dc}) is provided by renewable energy source such as solar power and /or energy storage systems. There is a feeder between DG and loads to flow current smoothly and the feeder contains only inductor however resistor is not added because it increases voltage distortion. Moreover there are some complex load conditions such as balance/unbalanced and linear/nonlinear loads connected to PCC also.

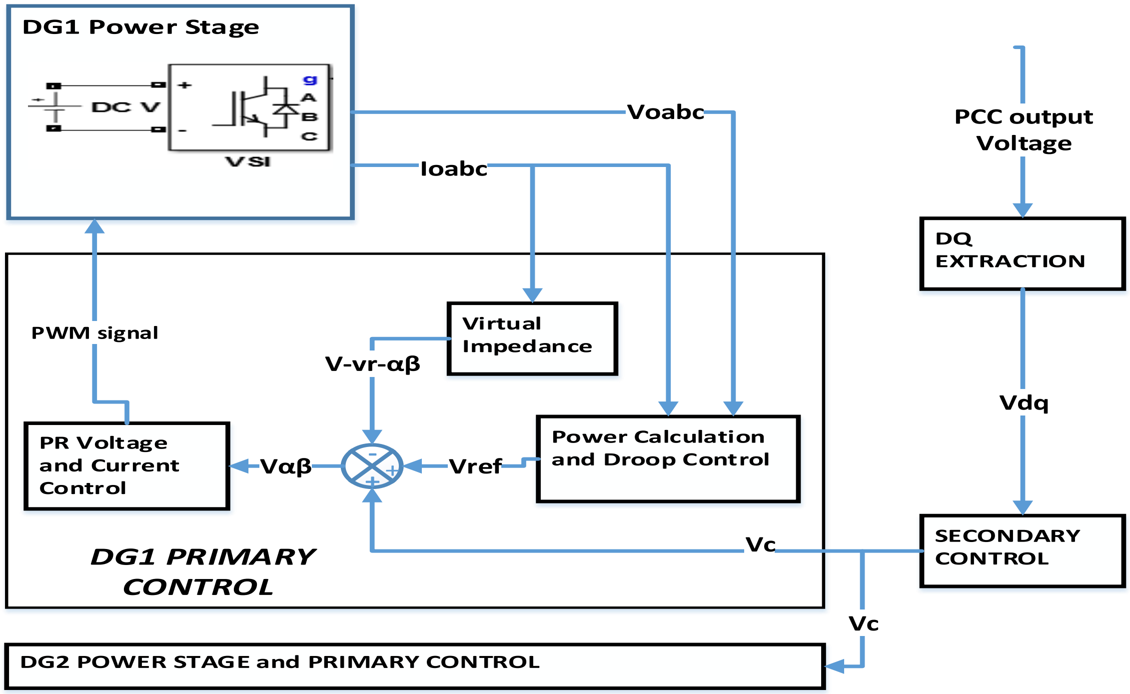

(a)

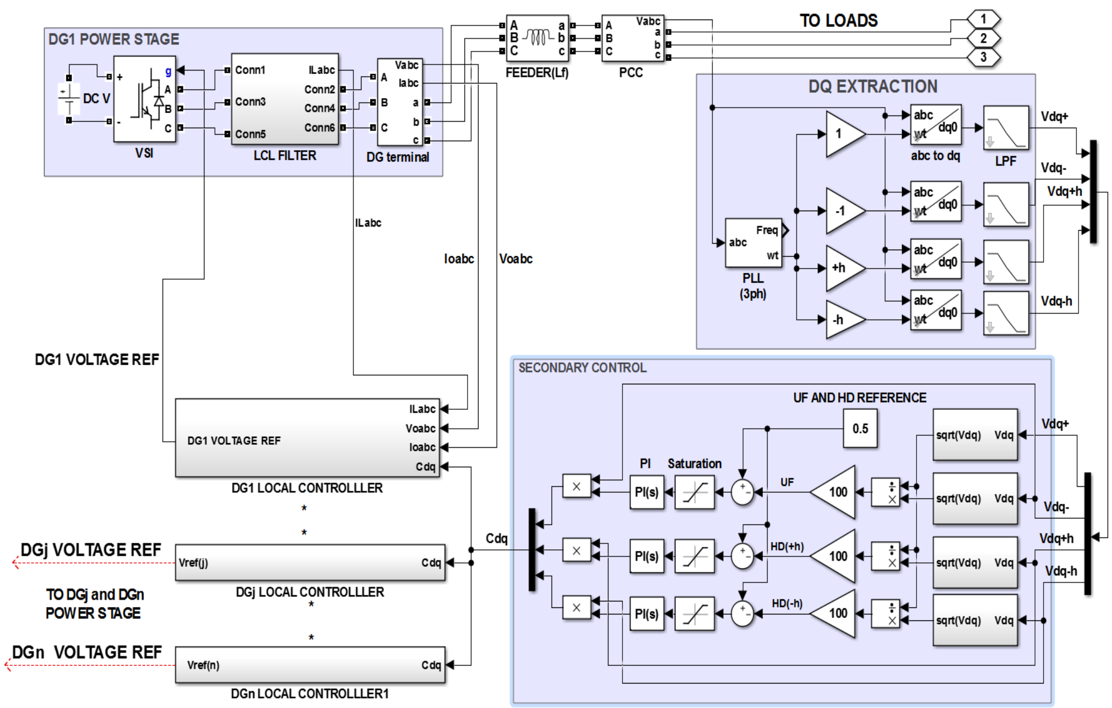

(b)

Fig 2.1. Power Stage and Hierarchical Control Scheme for the Proposed Micro Grid (a) Basic Block Diagram, (b) Simulink Model

Proposed hierarchical control consists of two control levels which are primary control level and secondary level for voltage source inverter (VSI) in microgrid applications in Fig 2.1 (a) and (b). In the control scheme, Secondary control manages compensation of positive and negative sequences of fundamental and main harmonic components for improving voltage quality. It sends proper reference signal to primary local control. Primary local control receives compensation voltage signal from secondary control and produces the reference voltage for DGs interface inverters. In the local controller of each DG in Fig 2.2 comprises power droop controller, current and voltage controllers controlled by proportional resonant (PR), and virtual impedance. In Fig 2.1 (b), PCC voltage unbalanced and harmonic data are extracted by dq extraction block to send PCC voltage information from dq components to secondary controller. In addition, secondary controller transmits compensation references of voltage unbalance and harmonic components to all DG primary controller. It is worth noting that the normal mode for triple harmonics is to be zero sequence. However unbalanced load will be added so 3th harmonic for positive and negative sequence compensation will be considered, in addition negative sequence compensation of 5^{th} and 11^{th} harmonics and negative sequence compensation of 7^{th} harmonics (the main orders) of PCC voltage are concerned in this thesis.

It should be noted that static switch can be disconnected from utility grid during main grid faults. In grid connected mode, main grid may also cause voltage distortion. Although proposed method can operate in both grid which are islanded mode and grid connected. In this research project, only islanded mode will be considered.

2.1. DG Primary Local Control System

The detailed structure of the DG1 local controller is designed in Fig. 2.2 to share powers and in addition, adjusts the frequency and amplitude of the DG output voltage reference. Each DG local controller consists power droop controller, proportional resonant current and voltage controller to track non-dc variables and virtual impedance to achieve better power of reactive, unbalance and harmonics. Droop controllers are the core parts of primary control level. Since there might be power circulation between parallel DGs, these controller are responsible for DG active and reactive power control. The main drawback of droop control is cannot nonlinear and unbalance load sharing. Therefore virtual impedance is used to share unbalance and harmonic current to provide resistance behavior toward harmonic components and the negative sequence of fundamental component of output current.

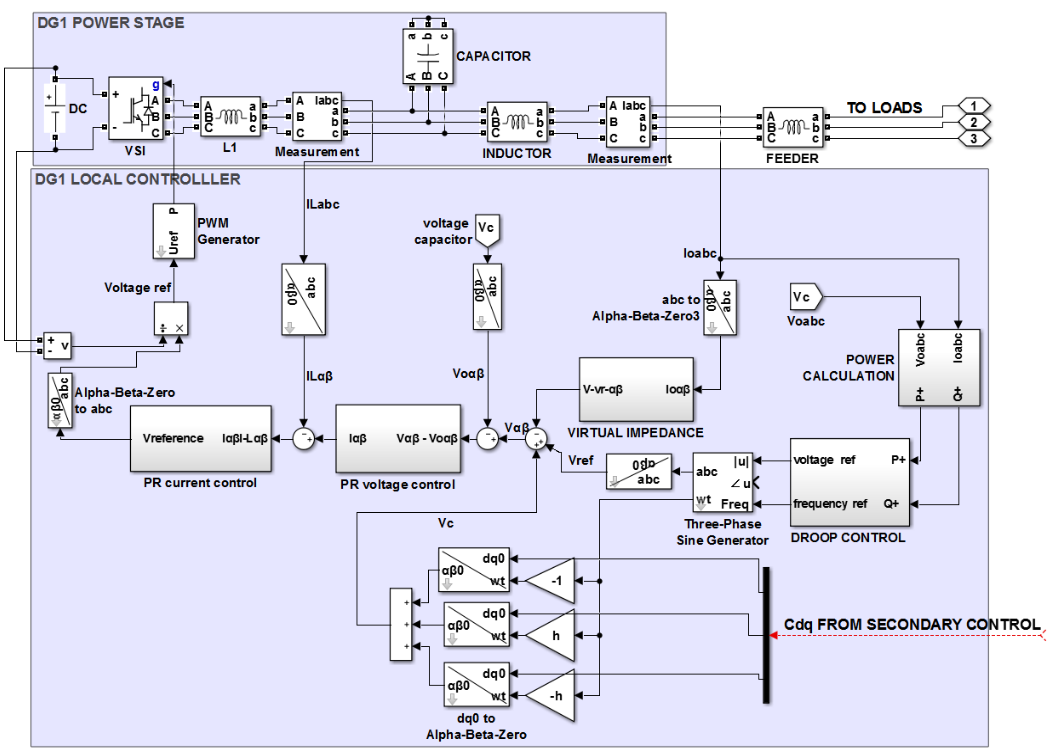

Fig 2.2. Detailed Block Diagram of DG1 Power Stage and Primary Local Controller

The local Dg controller is performed in αβ reference frame. Therefore, the Clarke transformation is used to transform the variables between abc and αβ frames. The equations (1) and (2) are used for the transformation:

$$x_{\alpha\beta} = \sqrt{\frac{2}{3}} \begin{bmatrix} 1 & \frac{-1}{2} & \frac{-1}{2} \\ 0 & \frac{\sqrt{3}}{2} & \frac{-\sqrt{3}}{2} \end{bmatrix} . x_{abc} \text{ and} \tag{2.1}$$

$$x_{abc} = \sqrt{\frac{2}{3}} \begin{bmatrix} 1 & 0 \\ \frac{-1}{2} & \frac{\sqrt{3}}{2} \\ \frac{-1}{2} & \frac{-\sqrt{3}}{2} \end{bmatrix} . x_{\alpha\beta}, \tag{2.2}$$

where $x_{\alpha\beta}$ and x_{abc} can represents the instantaneous output voltage ($V_{o\alpha\beta}$ and V_{oabc}), output current ($I_{o\alpha\beta}$ and I_{oabc}) or LCL filter inductor current ($I_{L\alpha\beta}$ and I_{Labc}) in αβ and abc frames respectively.

The stationary frame is converted by α and β components in (2.1) and (2.2). However zero component is not considered. In this thesis, a there phase three-wire islanded micro grid is considered. Since, zero sequence current cannot pass in the three-wire ungrounded electrical systems, zero sequence voltage drops will not affect the system voltages. Generally, zero sequence voltage cannot be present in the three-wire electrical systems in the absence of a fault (e.g., phase-to-ground short circuit) [21].

As shown in Fig 2.2, the reference of the DG output voltage in αβ frame ($V_{\alpha\beta}$) is provided by power controllers (V_{ref}), virtual impedance loop and secondary control (voltage compensation reference (V_c)). On the other hand, instantaneous output voltage (V_{oabc}) is measured and transformed to αβ frame ($V_{o\alpha\beta}$). Then, according to $V_{\alpha\beta}$ and $V_{o\alpha\beta}$, the reference current ($I_{\alpha\beta}$) is generated by voltage current control. LC filter inductor current (I_{Labc}) is transformed to αβ frame ($I_{L\alpha\beta}$) and controlled by the current controller. The output of the current controller is transformed back to abc frame to produce three phase voltage reference for pulse width modulator (PWM) block. Finally, PWM controls the switching of the inverter based on this reference.

2.1.1 Voltage Source Inverter (VSI)

Three phase pulse width modulation (PWM) inverter or voltage source inverter is widely used in microgrid and DG applications to convert DC input voltage to three phase AC voltages of variable magnitude as well as variable frequency using power electronic devices such as insulated gate bipolar transistor (IGBT) shown in Fig.2.3. In addition, PWM is supplied to set output voltage by changing pulse width and to set output frequency of circuit by changing modulation cycle [40-41]. However although PWM has rapid switching inherent to produce less harmonic distortion, the output of ac signal is still not sinusoidal and contains harmonics at 5th, 7th and other non-triple odd multiples of fundamental frequency. In order to reduce harmonic distortion, LCL filter are used as well. Three phase inverter consist three single phase half bridge inverters which has totally six IGBT switches (S1-S6) controlled by the switching variables as seen in Fig 2.3 The switches are turned on and turned off periodically and each switch conducts to each gate for 180° or for 120° in the proper sequence. In other words, gating signals are applied and removed at 60° intervals of the output voltage waveform [40-41]. For example, when two upper and one lower IGBTs or one upper and two lower IGBTs are switched on, the corresponding transistor are off to produce three phase Ac output voltage. Remember that the inverter switches such as S1 and S2 or S3 and S4 or S5 and S6 couples cannot be turned on or turned off at the same time to not make short circuit across the DC voltage. The switching frequency of the PWM in the inverter is 12 kHz for this research.

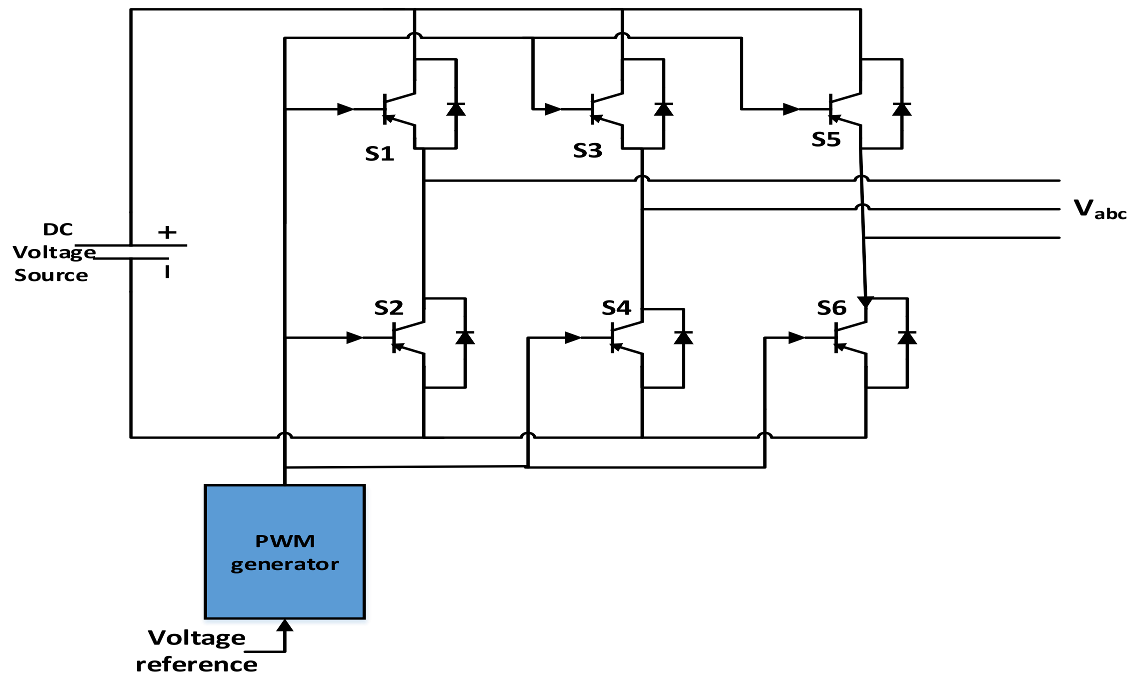

Fig 2.3 Three Phase Voltage Source inverter (VSI) circuit

2.1.2 Power Calculation and Modified Droop Control

Droop control strategy is the most used method for controlled the islanding microgrid with DG systems operating in parallel in order to share the total load demand to avoid DG overloads and to ensure stable operation of the microgrid. This concept stems from the power system theory, a synchronous generator reduces frequency, when the active power increases. The droop control can be integrated to VSI to mimic a synchronous generator principle.

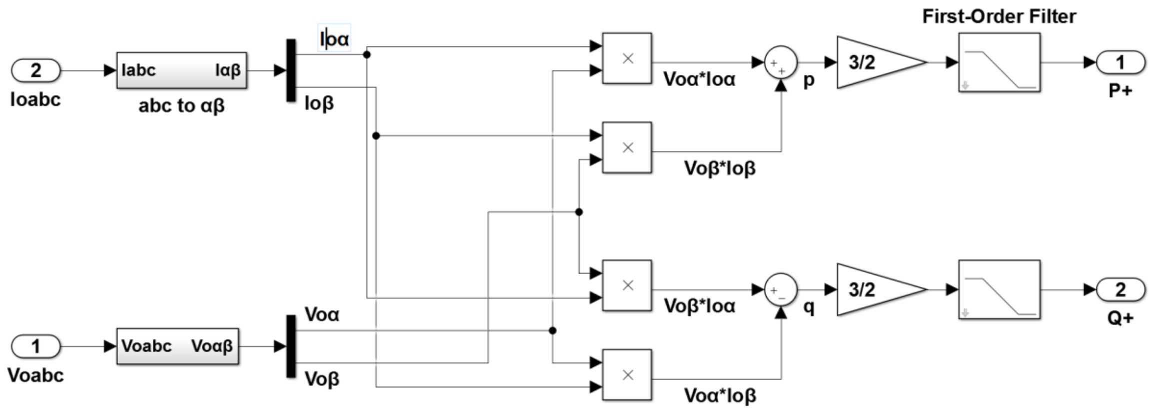

Fig 2.4 Block Diagram of Power Calculation

As seen in Fig 2.4, three phase instantaneous active power (p) and reactive power (q) can be calculated using output voltage ($V_{o\alpha\beta}$) and output current ($I_{o\alpha\beta}$) in $\alpha\beta$ refrence frame. The power equations can be expressed in (2.3) and (2.4) are

$p = v_{O\alpha}.i_{o\alpha} + v_{O\beta}.i_{o\beta}$ and (2.3)

$q = v_{O\beta}.i_{o\alpha} - v_{O\alpha}.i_{o\beta}$. (2.4)

Fundamental positive sequence power calculation is presented to extract dc components using two first order low pass filters (LPF). Dc components (average values of instantaneous active and reactive power) are positive sequence active and reactive powers (P+, Q+ respectively). Ac components are generated by the harmonic and unbalanced part of the voltages and currents powers.

Two first order LPFs with cutoff frequency of 2 Hz are used to extract the dc components. Note that if fundamental positive sequence components of voltage and current ($V^{+}_{\mathrm{o\alpha\beta}}$ and $i^{+}_{\mathrm{o\alpha\beta}}$ respectively) are used in (2.3) and (2.4) instead of output voltage output current ($V_{o\alpha\beta}$ and $I_{o\alpha\beta}$ respectively), dc components of powers can be calculated in another way. Thus, a low pass filter will not be necessary for power calculation.

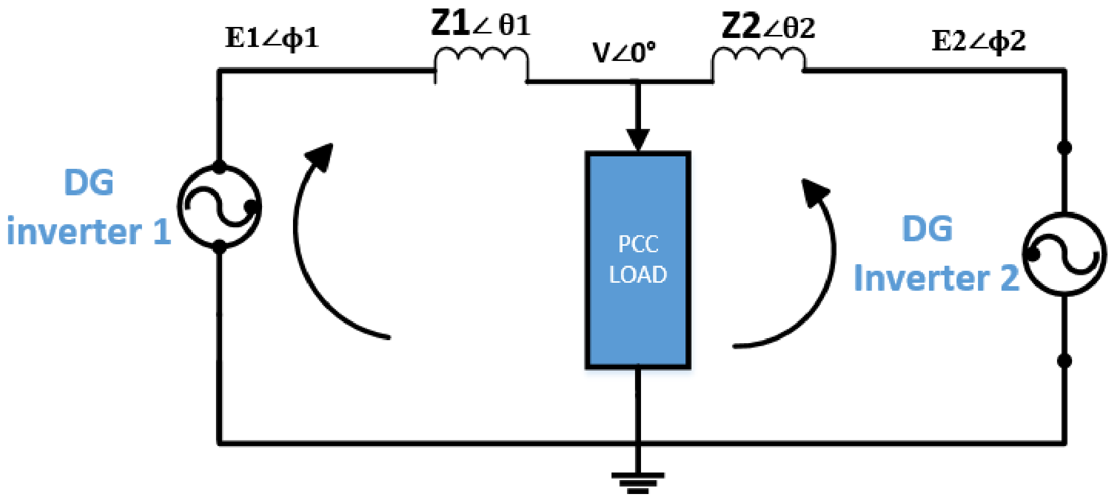

Fig 2.5 Equivalent Circuit of Two Parallel-Connected Inverters

Circulating of active and reactive power are shown in Fig 2.5, when two DG inverters or more are connected to PCC through the impedance Z∠θ. The active and reactive powers are injected to the grid by the DG [28]. Fundamental real and reactive powers can expressed in (2.5) and (2.6)

$$P = 3.\left(\frac{EV}{Z}\cos\emptyset - \frac{V^2}{Z}\right)\cos\emptyset \, + \, 3.\frac{EV}{Z}\sin\emptyset\sin\theta \text{ and} \tag{2.5}$$

$$Q = 3.\left(\frac{EV}{Z}\cos\emptyset - \frac{V^2}{Z}\right)\sin\emptyset \, + \, 3.\frac{EV}{Z}\sin\emptyset\cos\theta, \tag{2.6}$$

where E is magnitude of the inverter output voltage, V is the PCC voltage magnitude.$\emptyset$ represents the voltage phase angle difference (angle between E and V) and Z and θ are the magnitude and the phase of impedance between a DG and electrical grid, respectively. Assuming that phase of PCC voltage is zero, so the phase of the inverter voltage will be $\emptyset$.

In addition, considering mainly the impedance (Z) is inductive which means Z ≅ X θ=90. Moreover, the voltage phase angle difference ($\emptyset$) is performed very small (cosφ ≈ 1 and sinφ=φ) to improve system stability, thus P/Q decoupling in (2.7) and (2.8) can be simplified as:

$$P = 3.\frac{EV}{X}\sin\emptyset \text{ and} \tag{2.7}$$

$$Q = 3.\frac{V(E-V)}{X}. \tag{2.8}$$

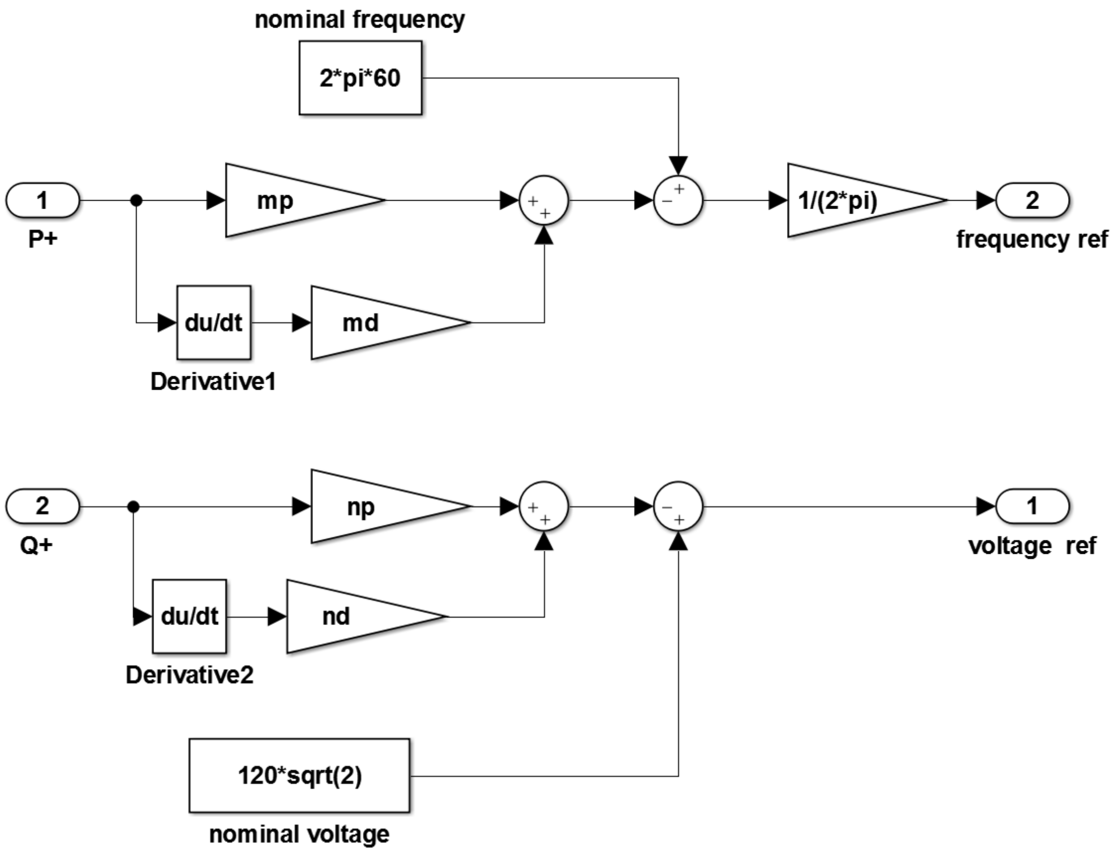

Fig. 2.6. Block Diagram of Droop Control

As a result, the droop control is adopted in Fig 2.6 to generate DG output voltage amplitude and frequency reference by adjusting fundamental positive active and reactive powers respectively in islanded micro grid. Afterwards, as can be seen in Fig 2.2, voltage reference is transformed to αβ reference frame to inject for DG voltage controller. Moreover, the droop control is applied to a DG inverter for sharing active and reactive power among DGs without communication in islanding micro grid. While frequency (in term of phase angle) is controlled by droop control in islanded operation, it is supported by main grid in grid connected operation.

According to this, the following droop control characteristics in Fig.2.5 are considered for DG output active and reactive powers in an islanding microgrid:

$$\omega^{*} = \omega_0 - P^{+}(\mathrm{m}_p + \mathrm{m}_d s) \text{ and} \tag{2.8}$$

$$E^{*} = E_0 - Q^{+}(\mathrm{n}_p + \mathrm{n}_d s), \tag{2.9}$$

where

E_0 : Nominal (rated) voltage amplitude

φ_0 : Nominal (rated) phase angle ($\int \omega_0 dt = \omega_0 t$)

ω_0 : rated angular frequency

m_p : Active power proportional coefficient

m_d : Active power derivative coefficient

n_p : Reactive power proportional coefficient

n_d : Reactive power derivative coefficient

E^{*} : Voltage amplitude reference

ω^{*} : Voltage frequency reference

P^{+}: Positive sequence active power

Q^{+}: Positive sequence reactive power.

It should be noted that nominal (rated) voltage amplitude and frequency reference are set 120 volt phase rms voltage and 60 Hz respectively and while Pref and Qref parameter are used in grid connected mode of microgrid, Pref and Qref must be set to zero in the islanded of MG, because only DGs supply the source to load in this mode. Moreover, DG units is equal capacities so droop control parameters are the same for all DG units.

The dynamics and the stability of the DGs is determined by power calculation filters and droop control [22]. Conventional droop control has several problems. For example, instability is caused by damping and oscillatory phenomena of phase shift difference and a transient current may overload and effect the unit negatively so systems do not arrives steady state fast. On the other hand, modified droop control is improved by adding transient droop characteristic to conventional droop approach to develop the transient response and reduces the circulating current among the DG units, in addition developing dynamic performance of the paralleled-system. Furthermore, the stability and good transient response can guarantee by selecting proportional (mp)-derivate (md) parameters and also equation (2.8) acts as proportional-derivate controller. Transient of the paralleled inverter system is improved by derivative term [23]. Adding and increasing np regulates reactive power sharing. Remember that in equation (2.9), no integral term is considered in reactive power droop characteristic. Because if integrators are used in islanded mode of MG, the load cannot coincide with total injected power and in addition reactive power is shared exactly. Therefore the system become unstable. However, in grid-connected mode they can be applied to share active and reactive power.

It is well known that good power sharing is achieved at the expense of degrading the voltage regulation, when droop coefficients are increased. However it can be acceptable, if the frequency and amplitude deviations are at 2% and 5%, respectively. Increasing of droop coefficients may damage transient response of the system, power sharing accuracy, and system stability [25].

Proportional power sharing, voltage quality, and stability should be considered to design the droop gains (mp, np, md) properly. When choosing the proportional P-ω droop coefficient mp, the real power sharing is guaranteed among DGs according to their power ratings and the coefficient md should be designed for a better dynamic response. But, there is a tradeoff between the reactive power accuracy and the voltage deviation which should be limited in the feasible range [26].in Table 2.1 power controller parameters are set according to above suggestions Note that if feeder or line impedances are difference, accuracy of reactive power sharing is low.

Table 2.1 Power Droop Controller Parameters for DG1and DG2

Power Controller (DG1/DG2)	
Active power proportional coefficient (m_p)	2e-4 (rad/W)
Active power derivative coefficient (m_d)	2e-5 (rad/W)
Reactive power proportional coefficient (n_p)	1e-3 (rad/W)
Reactive power derivative coefficient (n_d)	1e-4 (rad/W)

2.1.3 SOGI Based Virtual Impedance Loop

Modified droop control is not sufficient for DG(s) for nonlinear and unbalance load sharing and to share fundamental positive reactive power proportionally. Reactive, unbalance and harmonic powers also should be shared among DGs. Therefore, virtual impedance is implemented to share unbalance and harmonic current, to reduce voltage unbalance and harmonics distortion and for sharing reactive power better. It is noteworthy that positive and negative sequences of harmonic components should be regarded in virtual impedance since unbalance load condition is considered in the system.

Droop control deteriorates power sharing if the sum of the output impedance and the line impedance is unbalanced. To solve this, interface inductors can be included between the inverter and the load bus, but they are heavy and bulky. Therefore, as another solution, a virtual impedance loop has also been added to the voltage reference in order to fix the output impedance of the DGs by emulating lossless resistors or reactors [22]-[28].

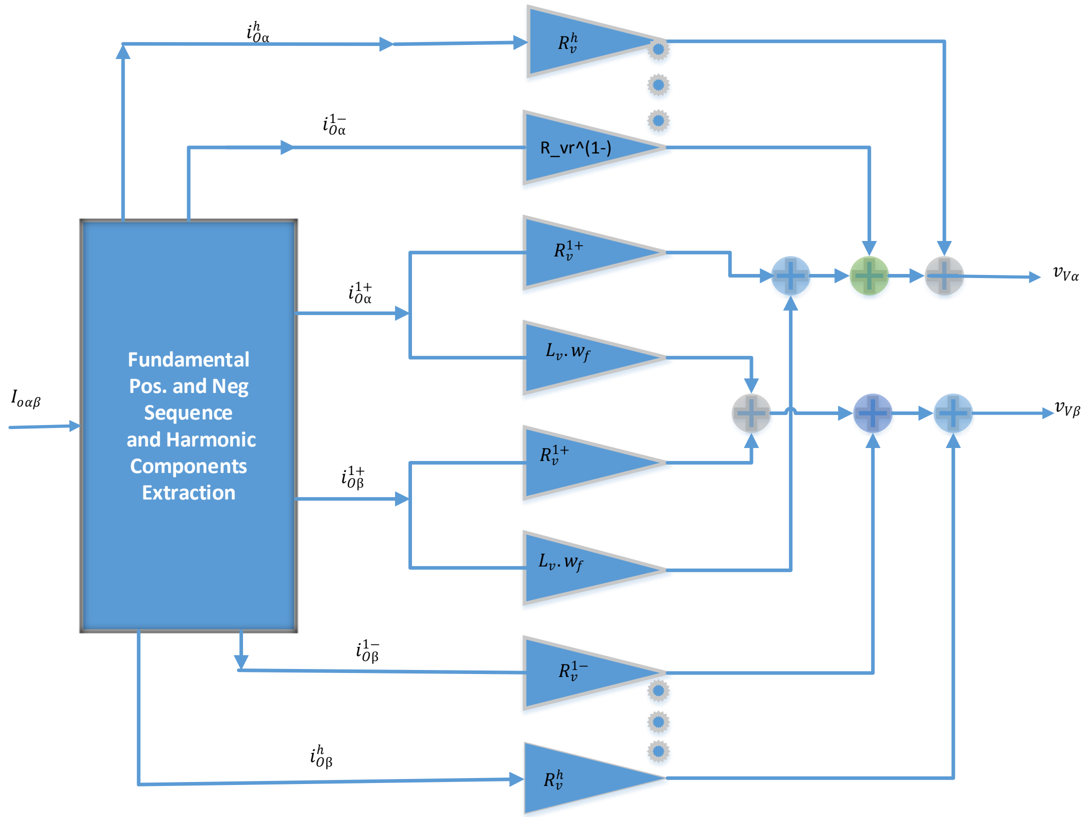

Fig. 2.7. Block Diagram of Virtual Impedance Control

Virtual impedance comprises three impedance loops which are virtual positive sequence impedance (VPI) at fundamental frequency, virtual negative sequence impedance (VNI) at fundamental frequency and virtual variable harmonics impedance (VVHI). Furthermore, only VPI loop has virtual inductance and resistance.

Virtual inductance makes output impedance more inductive to enhance decoupling of active (P) and reactive (Q) powers, and reducing power oscillations and circulating currents and for enhancing the system stability. Furthermore, virtual resistance is utilized improve system damping without physical power loss [6-11]. Note that physical resistance can be used to reduce oscillations, however power loos will increase. VPI, VNI and VVHI loops can be extracted in αβ reference frame in (7), (8) and (9)

$v_{V\alpha}^{1+} = R_v^{1+}.i_{O\alpha}^{1+} - L_v^{1+}.\omega_f.i_{O\beta}^{1+}$ and $v_{V\beta}^{1+} = R_v^{1+}.i_{O\beta}^{1+} + L_v^{1+}.\omega_f.i_{O\alpha}^{1+}$ for VPI loop, (2.10)

$v_{V\alpha}^{1-} = R_v^{1-}.i_{O\alpha}^{1-}$ and $v_{V\beta}^{1-} = R_v^{1-}.i_{O\beta}^{1-}$ for VNI loop, (2.11)

$v_{V\alpha,h} = R_v^{h}.i_{O\alpha}^{h}$ and $v_{V\beta,h} = R_v^{h}.i_{O\alpha,\mathrm{h}}^{h}$ for VVHI loop, (2.12)

where $v_{V\alpha\beta}^{1+}$ and $v_{V\alpha\beta}^{1-}$ represent virtual voltage for fundamental positive and negative sequences in $\alpha\beta$ frame. Furthermore, $v_{V\alpha\beta,h}$ is virtual hth harmonic sequence (both positive and negative sequences) in $\alpha\beta$ frame and h denotes dominant harmonic components. In addition, R_v^{1+} and L_v^{1+} are virtual resistance and inductance for fundamental positive components, R_v^{1-} represents virtual resistance for fundamental negative components. Also R_v^{h} is virtual resistance and inductance for hth main harmonic components. Finally, ω_f and $\omega_{f,h}$ represent the system fundamental and hth main harmonic frequencies. The fundamental frequency value is selected nominal frequency value and there is very low difference with operating frequency which may lead instability between the control loops.

The presence of the high R/X ratio causes coupling between active and reactive powers, thus VPI at fundamental frequency is designed to be mainly inductive to improve real and reactive power sharing. VNI at fundamental frequency is implemented to be resistive to reduce effectiveness of fundamental negative sequence current among DGs. Finally, virtual VVHI is also for sharing harmonic power properly among DG units and the positive resistance should be larger for getting better harmonic power [10]. As shown in Fig. 2.7, all three impedance loops added together to generate Vvαβ (virtual voltage in αβ frames). For simulation test, virtual impedance control parameters are set in Table2.2.

Table 2.2 Virtual Impedance Control Parameter

Virtual impedance(DG1/DG2)		
Fundamental positive sequence	Resistance (R_v^{1+})	-0.4 Ω
	Inductance (L_v^{1+})	2 mH
Fundamental negative sequence	Resistance (R_v^{1-})	-0.4 Ω
	Inductance (L_v^{1-})	2 mH
Positive sequence of 3rd harmonic	Resistance (R_v^{3+})	2 Ω
Positive sequence of 7th harmonic	Resistance (R_v^{7+})	4 Ω
Negative sequence of 5th harmonic	Resistance (R_v^{5-})	4 Ω
Negative sequence of 11th harmonic	Resistance (R_v^{11-})	2 Ω
Positive sequence of 13th harmonic	Resistance (R_v^{13+})	2 Ω
SOGI	Gain(k)	1.4

The detailed structure of the second-order general integrator (SOGI) is designed and explained in Fig.8, Fig 2.9 and Fig2.10.SOGI is a frequency adaptive resonant filter to extract positive and negative sequences of fundamental and harmonic components for voltage and current from a distorted grid voltage in phase locked loop (PLL) algorithm [29]. The SOGI diagram shown in Fig 2.8 (a) can be expressed its transfer function as

$$S(s) = \frac{y(s)}{x(s)} = \frac{ws}{s^2+w^2}, \tag{2.13}$$

where w is the SOGI resonant frequency and this frequency value comes from droop control produced by (2.8) equation. In this way, SOGI acts as an ideal integrator at this frequency. So, the two in-quadrature output signals of a second order band pass filter (BPF) $i\hat{}\alpha$ and $qi\hat{}\alpha$ with the following transfer function can be achieved as shown in Fig.2.8 (b)

$$D(s) = \frac{i\hat{}\alpha}{i\alpha} = \frac{kws}{s^2+kws+w^2} \text{ and} \tag{2.14}$$

$$Q(s) = \frac{qi\hat{}\alpha}{i\alpha} = \frac{kw^2}{s^2+kws+w^2}, \tag{2.15}$$

where k is damping factor of the BPF, selected as k= 1.5. BPF looks like the low-pass filter, in which the static gain only depends on k.

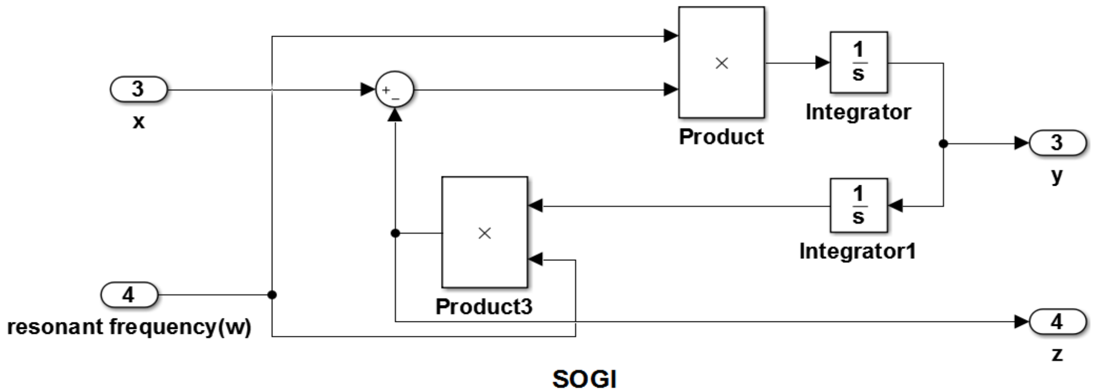

(a)

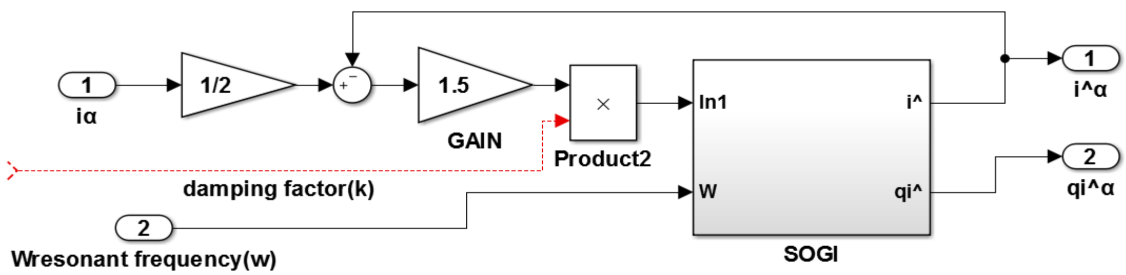

(b)

Fig 2.8. (a) SOGI Structure (b) BPF Block Diagram

As can be noticed, if w and k are selected properly, almost sinusoidal fundamental components of $i^\wedge\alpha$ will be provided. Higher k allows to pass other frequency, while for lower k value, filter is tighter around the resonance frequency. In addition, signal $qi^\wedge\alpha$ is always 90° lagged from the quadrature phase version of $i^\wedge\alpha$ for detection symmetrical components in three-phase systems [30].

The instantaneous positive- and negative-sequence current components on the αβ reference frame can be calculated as

$$i_{\alpha\beta}^{1+} = \frac{1}{2}\begin{bmatrix} 1 & -q \\ q & 1 \end{bmatrix} . i_{\alpha\beta} \text{ and} \tag{2.16}$$

$$i_{V\alpha\beta}^{1-} = \frac{1}{2}\begin{bmatrix} 1 & q \\ -q & 1 \end{bmatrix} . i_{\alpha\beta}, \tag{2.17}$$

where $q = e^{-j\frac{\pi}{2}}$ as a shift operator in the time domain which obtains the quadrature-phase waveform (90° lagged) of the original in-phase waveform. In Fig.2.7, i_α and i_β instantaneous output currents are calculated by abc to αβ transform block and through double SOGIs (DSOGI), the instantaneous positive- and negative output current on the αβ reference frame can be obtained.

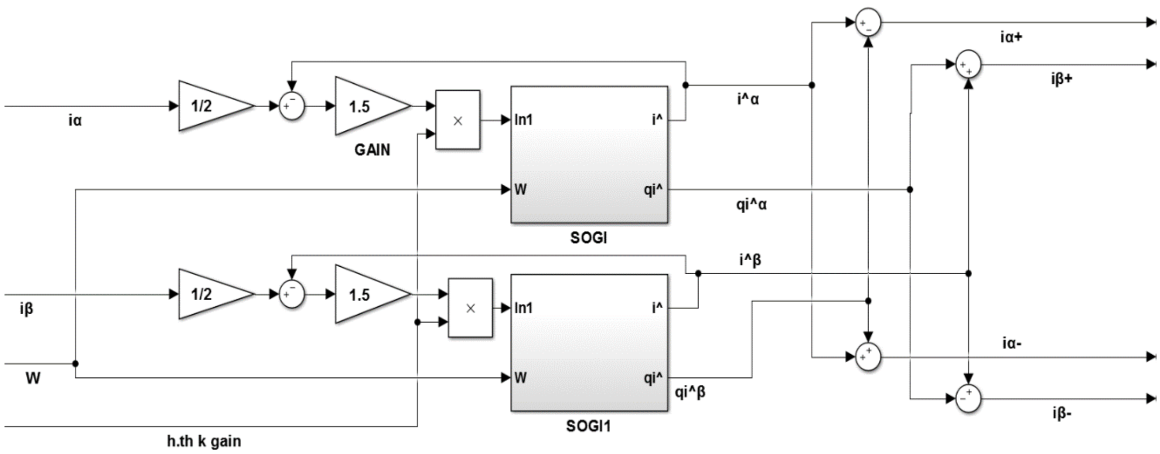

Fig 2.9. Block Diagram of DSOGI for Extracting the Positive and Negative Sequences

To detect multiple harmonic components from an unbalanced and distorted three-phase input current vector, several DSOGI blocks are tuned at different harmonic frequencies and connected each other by using the cross-feedback network in Fig. 2.10. The fundamental frequency is multiplied by the corresponding harmonic order to tune the rest of the DSOGI. Moreover, the value of n in each DSOGI is divided by the corresponding harmonic order to keep the product nω constant, which guarantees the same bandwidth for all the DSOGIs. Detail of MSOGI is presented in [30].

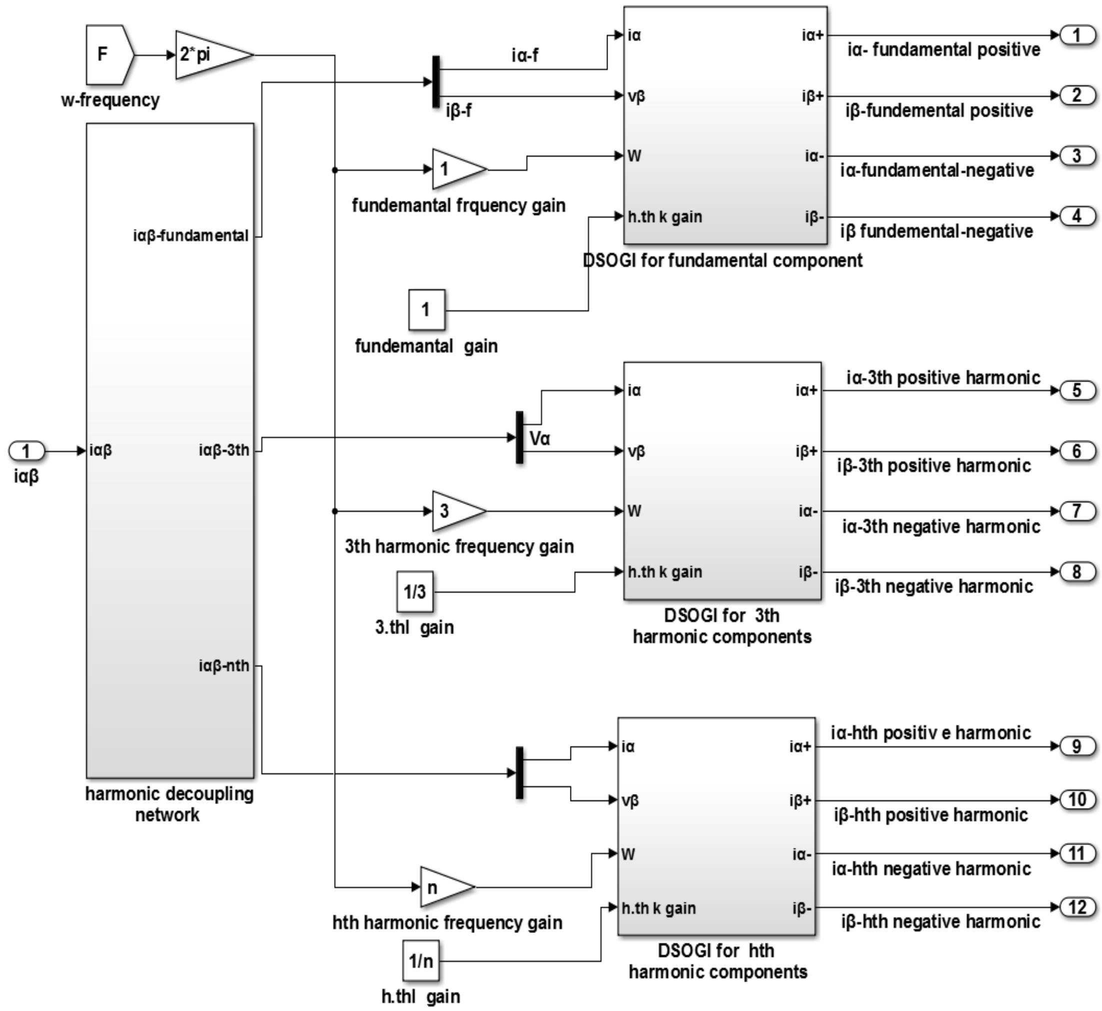

Fig 2.10 Block Diagram of MSOGI to Extract Positive and Negative Sequences of Fundamental and Harmonic Components

2.1.4 Proportional Resonant (PR) Current and Voltage Controller

The primary level is a local controller, which consists of voltage and current inner control loops in order to fix the filter capacitor voltage and the inductance current. Proportional resonant current and voltage controller are implemented to follow non-dc variables and control the voltage and the current in the stationary frame [6].

Compared with PI control, PR voltage and current can provide larger gain at the fundamental frequency and no phase shift and gain at the other frequencies to eliminate the steady-state error to reduce the sensitivity of the compensator to variations at the fundamental frequency [32]. An ideal PR controller which can give stability problems because of the infinite gain. To overcome that problem, damping (cut-off frequency) added to the controller to be non-ideal. PR voltage and current controllers are as (10) and (11):

$$G_V(s) = k_{pV} + \sum_{k=1,3,5,7} \frac{2k_{rVk}.\omega_{cV}.s}{s^2+2.\omega_{cV}.s+(k.\omega_0)^2} \text{ and} \tag{10}$$

$$G_I(s) = k_{pI} + \sum_{k=1,3,5,7} \frac{2k_{rIk}.\omega_{cI}.s}{s^2+2.\omega_{cI}.s+(k.\omega_0)^2}, \tag{11}$$

where k_{pV} (k_{pI}) is the proportional coefficient of the voltage (current) controller and k_{rVk}(k_{rIk}) represents the kth harmonic (including fundamental sequence as first harmonic) resonant coefficient of the voltage (current) controller. k_{pV} and k_{pI} term determines the dynamics of the system, bandwidth, phase and gain margins. In addition, ω_{cV} and ω_{cI} are cut-off frequency of the voltage and current controllers which are the bandwidth around the ac frequency ofω_0, respectively. In (10) and (11) equation, non-ideal resonant provide a wider resonant peak, therefore is less sensitive to frequency fluctuations. The gain at resonant frequency is finite, however, still high enough to ensure a small tracking error [24].

In addition, it is simple to extend the capabilities of the scheme by adding harmonic sequence at desired harmonic sequences (3^{th}, 5^{th}, 7^{th}) with more resonant controllers in parallel to the main controller PR controllers to suppress voltage harmonics and to track harmonic current and voltage. Note that desired harmonic components do not have to be positive and negative sequences in this controllers. Thus only one is enough for compensation and also do not affect the dynamics of the PR controllers. To design optimal parameter for the control, k_r at the desired frequency should be high to achieve small steady state error and to provide sufficient bandwidth, k_p should be set [33].

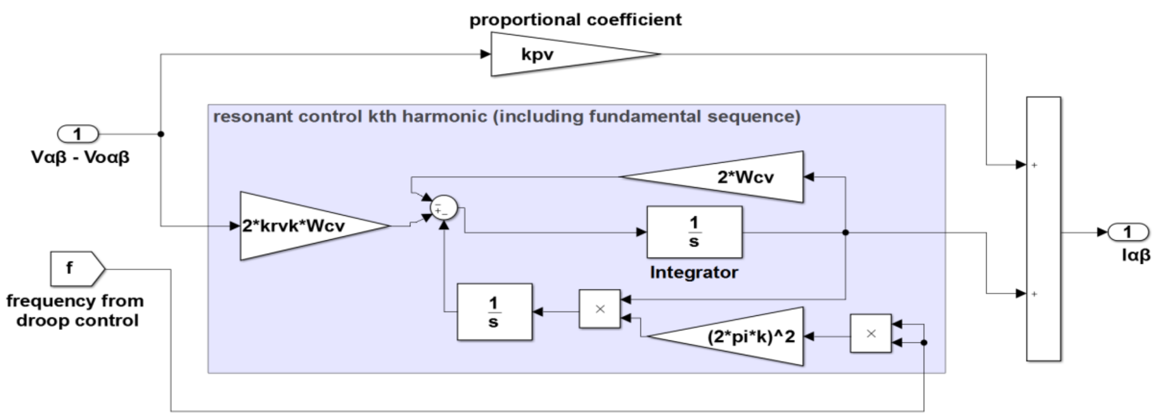

Fig.2.11. Block Diagram of Proportional Voltage Control

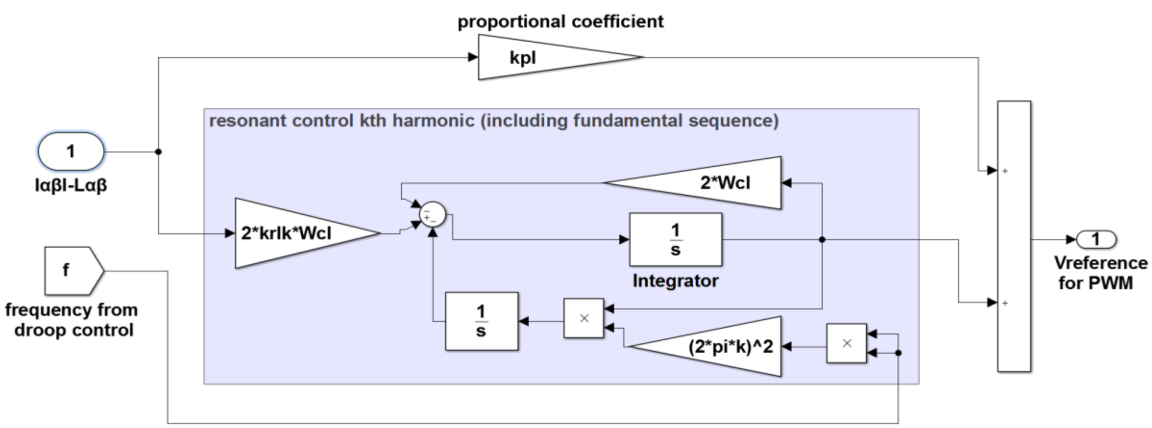

Fig 2.12. Block Diagram of Proportional Current Control

As seen in Fig. 2, the reference of the Dg output voltage ($V_{\alpha\beta}$) is provided by power droop control and virtual impedance and secondary control. Then it is compared with measured instantaneous inverter voltage ($V_{o\alpha\beta}$) for voltage PR voltage controller in Fig.2.11 to generate reference current ($I_{\alpha\beta}$). On the other hand, measured inverter inductance current (I_{Labc}) from LC filter is transformed to αβ reference frame. Both currents ($I_{\alpha\beta}$ andI_{Labc}) are regulated by PR current controller in Fig.2.12. Finally, output of current controller is transformed back to abc frame to produce three phase voltage reference for pulse width modulator (PWM) signals to generate output voltage of inverters.

Table 2.3 Proportional Resonant Voltage/Current Controller Parameters

PR Voltage/Current Controller (DG1/DG2)	
Proportional coefficient (k_{pV} /k_{pI})	1 / 20
Fundamental resonant coefficient ($\mathrm{k_{rV1}}$/ $\mathrm{k_{rI1}}$)	100 / 1100
3th harmonic resonant coefficient ($\mathrm{k_{rV3}}$/$\mathrm{k_{rI3}}$)	200 / 400
5th harmonic resonant coefficient ($\mathrm{k_{rV5}}$/ $\mathrm{k_{rI5}}$)	30 / 55
7th harmonic resonant coefficient ($\mathrm{k_{rV7}}$ / $\mathrm{k_{rI7}}$)	1.5 / 7.5
11th harmonic resonant coefficient ($\mathrm{k_{rV11}}$/ $\mathrm{k_{rI11}}$)	1 / 5
13th harmonic resonant coefficient ($\mathrm{k_{rV13}}$ / $\mathrm{k_{rI13}}$)	1 / 5
Cut-off frequency (ω_{cV}/ω_{cI})	2 / 2

Magnitude and phase bode diagram of voltage and current proportional control in open loop are depicted in Fig.2.13 and Fig.2.14. As shown, in both magnitude graph, the gains are high at fundamental and 3th, 5th and 7th harmonics frequency to reach zero steady state error. In addition, to have less sensitive frequency fluctuations, wider resonant are chosen high value. In phase diagram, 90 degree (negative) phase shift occur at fundamental and 3th, 5th and 7th harmonics frequency. As a result, the parameters of proportional resonant voltage / current controllers are listed in Table 2.3 for simulation test.

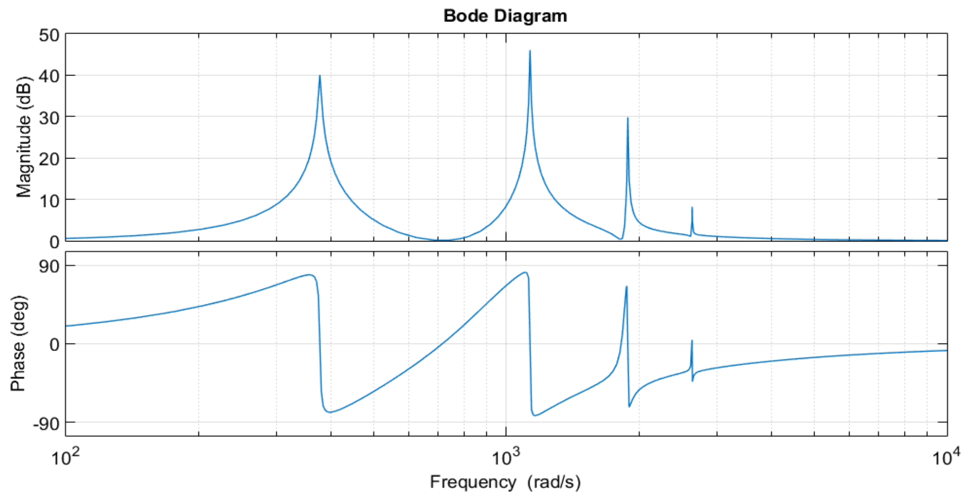

Fig 2.13 Bode Plot of Voltage Proportional Controller

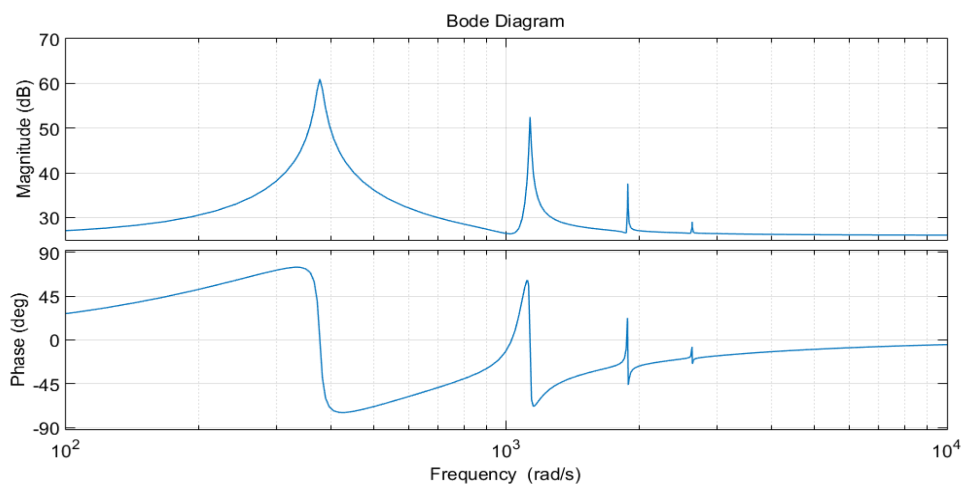

Fig 2.14 Bode Plot of Current Proportional Controller

To calculate close loop transfer function and output impedance, the diagram of the Voltage and Current Controller with Virtual Impedance Control Simplified in Fig 2.15. The voltage reference of a DG unit in αβ frame ($V_{\alpha\beta}$) is modified by power controllers (V_{ref}), virtual impedance loop and voltage compensation reference signals. The output voltage of capacitance can be provided as follow:

$$V_{o\alpha\beta} = G(s)(V_{\alpha\beta}) - (G(s)Z_{V\alpha\beta}(s) + Z_{o\alpha\beta}(s))I_{o\alpha\beta}, \quad (12)$$

where $G(s)$, $Z_{V\alpha\beta}(s)$ and $Z_{o\alpha\beta}(s)$ are the close loop transfer function of local control, virtual impedance ($Z_{V\alpha\beta}(s) = R_v + L_v$) and the output impedance without impedance loops, respectively VNI is omitted because it is only for attenuating circulation current [10]. Note that for positive negative sequence, virtual impedance loop is only considered as seen in Fig 2.15, in addition, it is necessary to replace s by "–s'' for negative sequence. The close loop transfer function and the output impedance without impedance loops can be derived as

$$G(s) = \frac{G_V(s)G_I(s)}{L_1Cs^2 + (Cs + G_V(s))G_I(s) + 1} \text{ and} \quad (13)$$

$$Z_{o\alpha\beta}(s) = \frac{Ls + G_I(s)}{L_1Cs^2 + (Cs + G_V(s))G_I(s) + 1}. \quad (14)$$

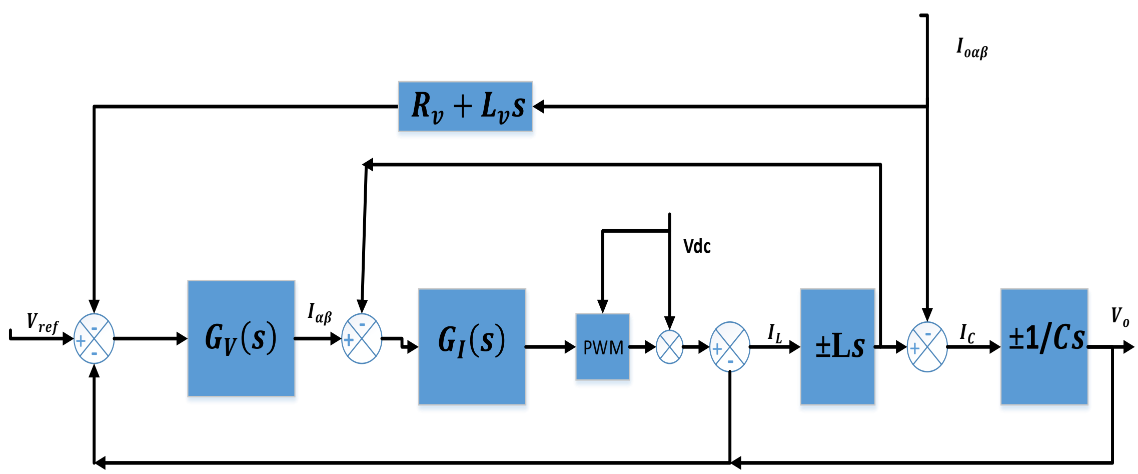

Fig 2.15 Simplified Diagram of the Voltage and Current Controller with Virtual Impedance Control

2.2. Secondary Control

Dq components extraction of measured PCC voltage and secondary control are depicted in Fig.2.1 to extract unbalanced and harmonic components. Signs of "+", "-", ""and "h" represent positive and negative sequence of fundamental component and hth harmonic component, respectively. For example "v_{dq}^{1-}" is negative sequence of fundamental voltage in dq frame. PLL is used to estimate voltage frequency and angular position of rotation frame (ω). To transform v_{abc} to v_{dq}, the rotation frame is multiplied by positive and negative sequence of fundamental component and selected hth harmonic component gain which represent 1, -1, +h, -h respectively. The park transformation is used to transform the variables between abc and dq frames. The equations (2.1) and (2.2) are used for the transformation:

$$x_{\mathrm{dq}} = \sqrt{\frac{2}{3}} \begin{bmatrix} \cos \omega t & \cos(\omega t - \frac{2\pi}{3}) & \cos(\omega t + \frac{2\pi}{3}) \\ \sin \omega t & \sin(\omega t - \frac{2\pi}{3}) & \sin(\omega t + \frac{2\pi}{3}) \end{bmatrix} . x_{\mathrm{abc}} \text{ and} \tag{2.1}$$

$$x_{\mathrm{abc}} = \sqrt{\frac{2}{3}} \begin{bmatrix} \cos \omega t & \sin \omega t \\ \cos(\omega t - \frac{2\pi}{3}) & \sin(\omega t - \frac{2\pi}{3}) \\ \cos(\omega t + \frac{2\pi}{3}) & \sin(\omega t + \frac{2\pi}{3}) \end{bmatrix} . x_{\alpha\beta}, \tag{2.2}$$

where x represents a control variable and is ω the microgrid operating frequency. After dq extraction, Second order (2^{nd}) low-pass filter is applied with cutoff frequency of 5 Hz and damping ratio of 2.5 are used to extract positive and negative sequences of PCC voltage fundamental and main harmonic components in Fig.2.1. It should be noted that the first-order filter cannot provide acceptable performance to filter the oscillations, properly thus, second-order filters are applied [20].

Afterward, v_{dq}^{1-}, v_{dq}^{1+}, v_{dq}^{h+} and v_{dq}^{h-} are sent to secondary controller to reduce unbalanced voltage and harmonic distortion. Block diagram of secondary controller is depicted in Fig.2.1. v_{dq}^{1-}, v_{dq}^{1+}, v_{dq}^{h+} and v_{dq}^{h-} are used to calculate the PCC voltage magnitudes of the positive and negative sequence of fundamental component and selected hth harmonic component based on dq reference frame in Fig.2.16 and then the voltage unbalance factor (VUF) and positive and negative harmonic distortion indices (HD^{h+}, HD^{h-}) are calculated using following equation:

$$\%VUF = \frac{\sqrt{(V_d^{-1})^2+(V_q^{-1})^2}}{\sqrt{(V_d^{+1})^2+(V_q^{+1})^2}} x100, \tag{2.3}$$

$$\%HD^{h+} = \frac{\sqrt{(V_d^{+h})^2+(V_q^{+h})^2}}{\sqrt{(V_d^{+1})^2+(V_q^{+1})^2}} x100, \text{ and} \tag{2.4}$$

$$\%HD^{h-} = \frac{\sqrt{(V_d^{-h})^2+(V_q^{-h})^2}}{\sqrt{(V_d^{+1})^2+(V_q^{+1})^2}} x100. \tag{2.5}$$

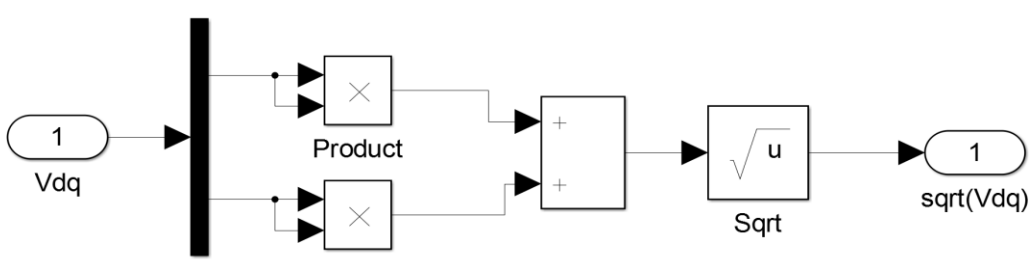

Fig 2.16. Block Diagram of Magnitude of Voltage dq Component

Then unbalanced factor and harmonic indices reference are compared to UF, HD^{h+} and HD^{h-} if there is any distortion. Note that if unbalanced factor and harmonic reference is less than PCC voltage distortion, saturation block must be used to not effect stability of control system. The error are fed to proportional control (PI) controller to reduce voltage unbalanced and harmonic distortion. Then each output of the PI controller of negative sequence of fundamental component and selected hth harmonic component is multiplied by v_{dq}^{1-}, v_{dq}^{h+} and v_{dq}^{h-} to produce C_{dq}^{1-}, C_{dq}^{h+} and C_{dq}^{h-} compensation references respectively which are transmitted to each primary local control to mitigate PCC distortion to the reference value.

As shown in Fig. 2.2, unbalanced and harmonic voltages are transformed to αβ (stationary) reference frame and added to DG local control. The angular position of rotation frame are set to -φ and -hφ and hφ for the unbalanced, (h+)th and (h-)th harmonics, respectively. wt is the reference of DG voltage angular position which is generated by the active power controller.

As aforementioned, negative sequence of fundamental component, 3th harmonic for positive sequence compensation will be considered, in addition positive and negative sequence compensation of 5^{th}, 7th and 11^{th} harmonics (the main orders) of PCC voltage is concerned for PI control. In addition, PI control should be tuned considering the required power quality and the possible practical limitations and to reduce response time by increasing proportional coefficient of PI controller. However the control system may become unstable [9]. To avoid these problem, the parameters of PI controllers are adjusted in Table 2.4. It should be noted that secondary controller transmits compensation references of voltage unbalance and harmonic components to all DG primary controller.

Table 2.4 Secondary PI Controllers Parameters

Fundamental negative sequence		3rd Harmonic positive sequence	
proportional	integral	proportional	integral
0.6	6	0.1	0.7
5th Harmonic negative sequence		7th Harmonic positive sequence	
proportional	Integral	proportional	integral
2.5	30	2.5	30
11th Harmonic negative sequence		13th Harmonic positive sequence	
proportional	Integral	proportional	integral
2	20	0.5	5

CHAPTER 3 SIMULATION RESULTS

The test system of proposed islanded micro grid is demonstrated in Fig. 3.1 test system consists of a linear load, an unbalanced resistive load and a nonlinear load and two DG units with power stage and control system in Figs. 1.1-1.2. Unbalanced load of a single phase is connected to PCC between phases a and b to create unbalance distortion. Furthermore, a nonlinear load with diode rectifier also connected to PCC and each DG unit will be the same power rating. In addition, power stage, loads, power droop controller virtual impedance controller, PR voltage/current controller and secondary PI control parameters are given in Table 3.1- 2.1- 2.2 2.3 and table 2.4 respectively to simulate the control system under an unbalanced load and a nonlinear load. VUF and HD reference value are set to %0.5. Switching frequency of the DGs unit will be set 12 KHz. Proposed method is implemented on MATLAB/Simulink.

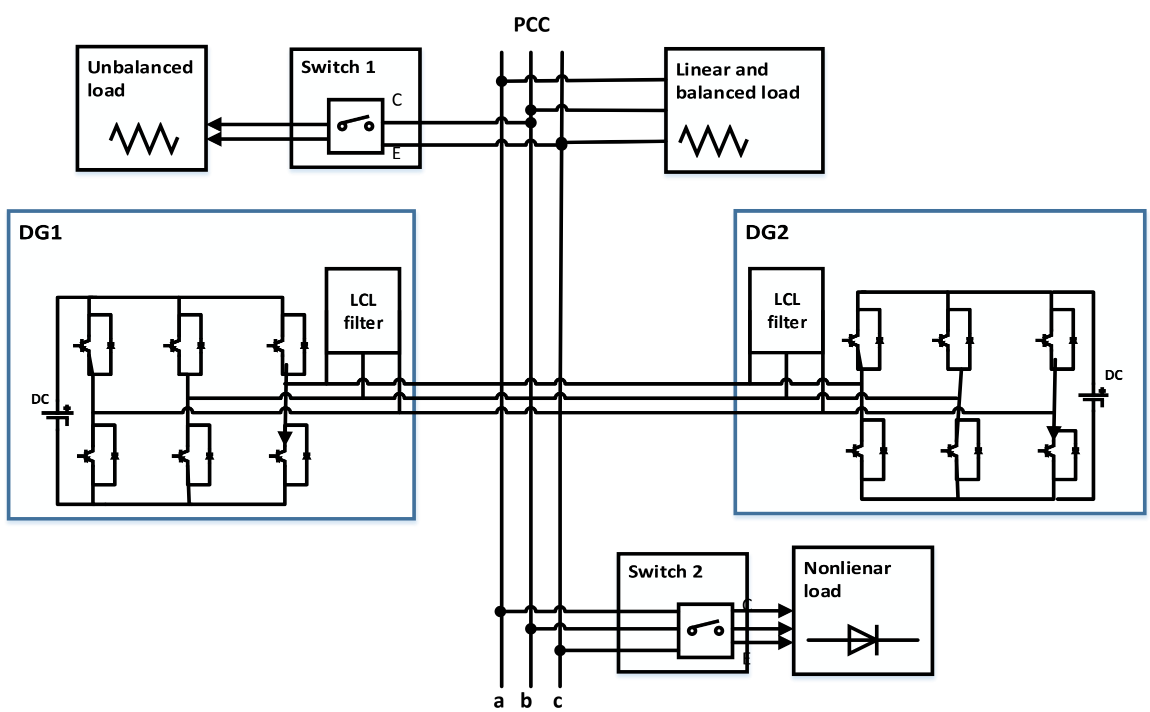

Fig. 3.1 Schematic of the Test System with Two Parallel Connected DG Units

Table 3.1 Power Stage and Loads Parameter

Parameter	**DG1/DG2**	**Linear load**	
DC link voltage (V_{dc})	400 V	Resistance(R_L)	10 Ω
Switching frequency (f_{sw})	12 kHz	Inductance(L_L)	2e-3 mH
Inverter side inductor (L1)	1.8 mH	**Unbalanced load**	
Inverter side inductor (C)	25 μF	Resistance(R_{UL})	10 Ω
Inverter side inductor (L2)	1.8 mH	**Nonlinear load**	
Feeder inductor (Lf)	1.8 mH	Resistance(R_{NL})	30 Ω
Nominal voltage amplitude (E_0)	120 rms V	Inductance(L_{NL})	84e mH
Nominal angular frequency (ω_0)	2*pi*60 (rad/s)	Capacitance (C_{NL})	235e μF

The effectiveness of the proposed control scheme in simulations are considered in three steps. In first step with unbalanced load connected to PCC, switch1 is closed mode and switch2 is open state to test unbalanced voltage quality. Second step with nonlinear load connected to PCC is that switch2 is closed mode and switch1 is open state to demonstrate reduction of harmonic voltage. Finally, both switches are closed in third step to observe improving of power quality voltage under unbalanced and nonlinear loads. Note that there is no any switch for linear load. Thus for all steps, the linear load will be active.

Three steps can be shown as: Step 1 is that switch1 is closed and switch2 is open. Only Droop control and virtual positive and negative impedance and secondary control for unbalanced load compensation are activated. Step 2 is that switch1 is open and switch2 is closed. Droop control and virtual positive and virtual harmonic impedance and secondary control for main harmonic compensation are performed. Step 3 is that switch1 and switch2 are closed. Droop control and all virtual impedance and secondary control for unbalanced and nonlinear voltage compensation are acting.

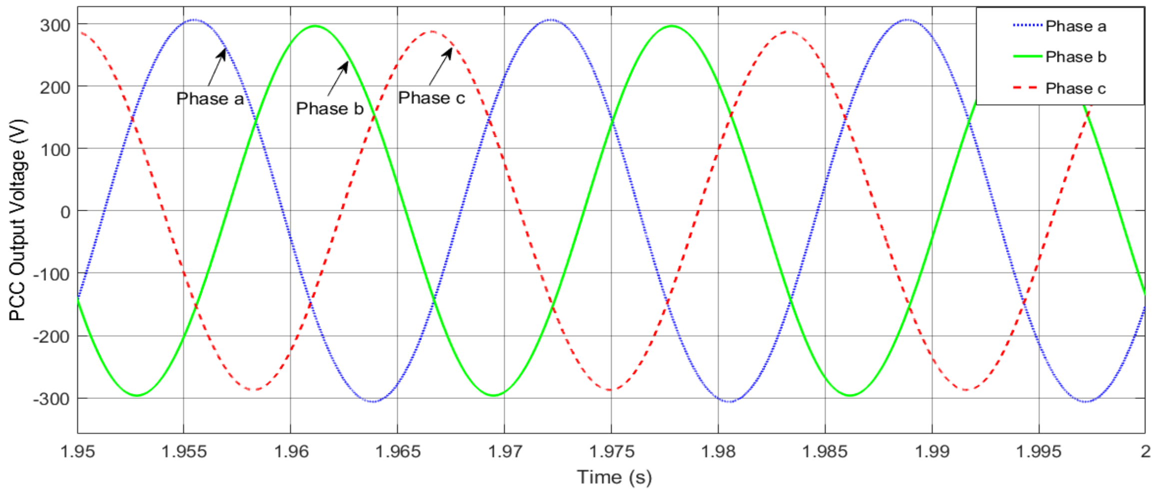

(a) Output Voltages of PCC

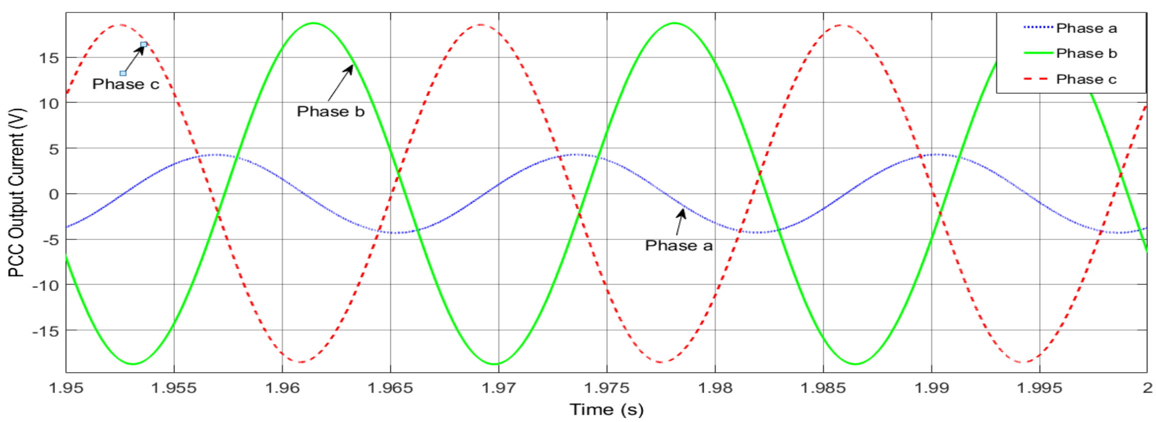

(b) Output Currents of PCC

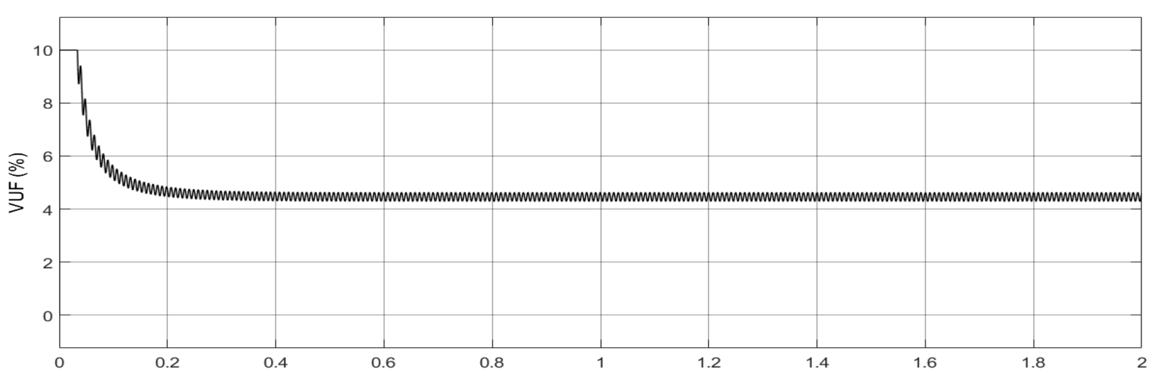

(b) VUF at PCC

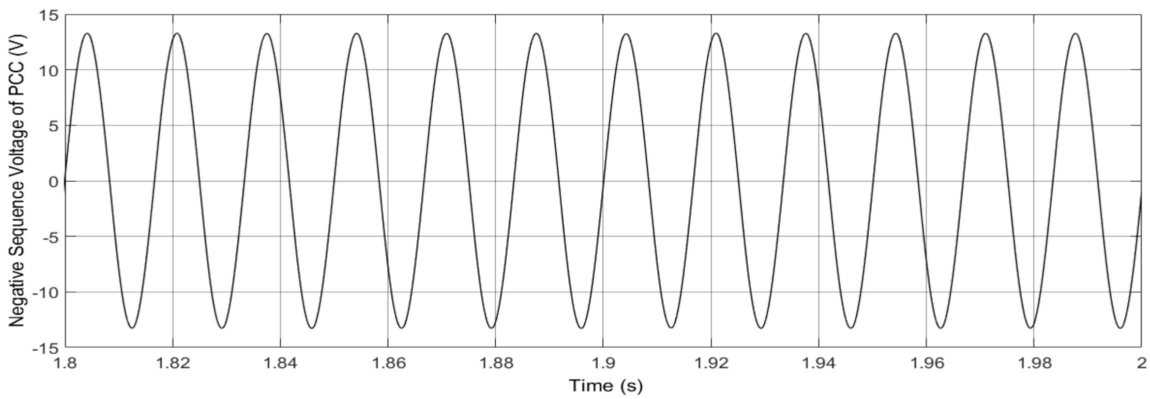

(d)

Fig 3.2. Performance of the Conventional Droop Control in a Microgrid with Unbalanced Load. (a) Output Voltages of PCC. (b) Output Currents of PCC. (c) VUF at PCC (d) Phase-a Negative Squence Voltage of PCC

3.1. Results under Unbalanced Load for Step 1

Before activating unbalanced compensation method, droop control and virtual positive impedance in microgrid with unbalanced load are implemented and switch1 is closed mode and switch2 is open state. Fig 3.2 (a) shows that PCC voltage are unbalanced which means that magnitude of the voltage is not equal. In addition, PCC current is not shared equally and as phase a of PCC load is disconnected, it can be seen that higher circulating component appears between the phase c of PCC in Fig 3.2 (b). In Fig.3.2 (c), it can be seen that unbalance factor is high and VUF values is %4.5. Moreover, Fig.3.2 (d) depicts that single negative squence of fundamental voltage at PCC is high.

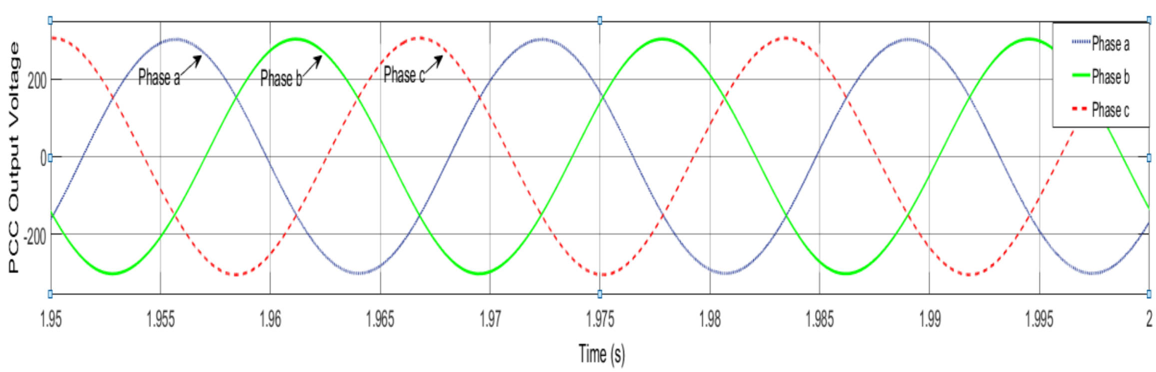

(a) Output Voltages of PCC

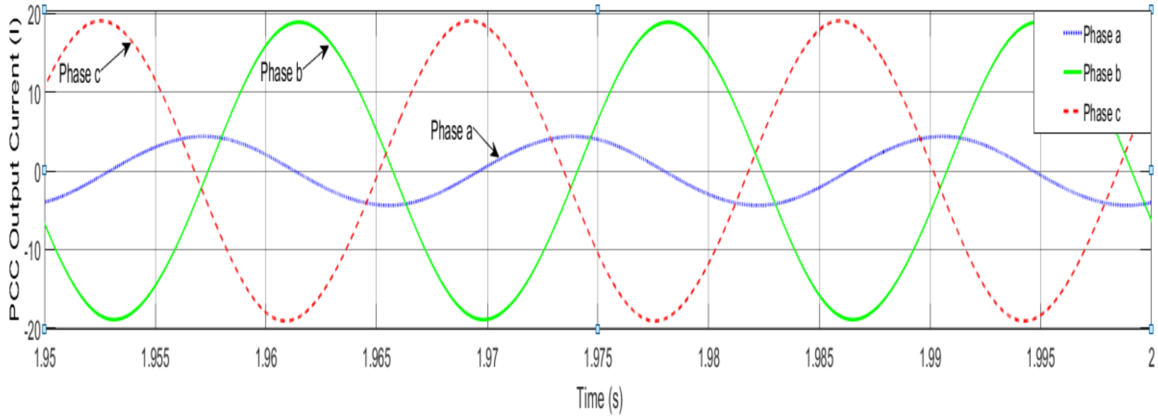

(b)

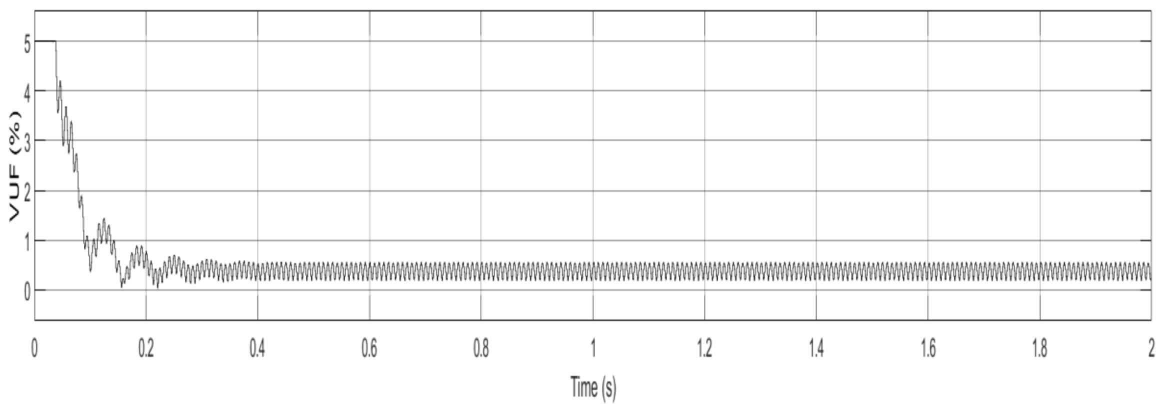

(c)

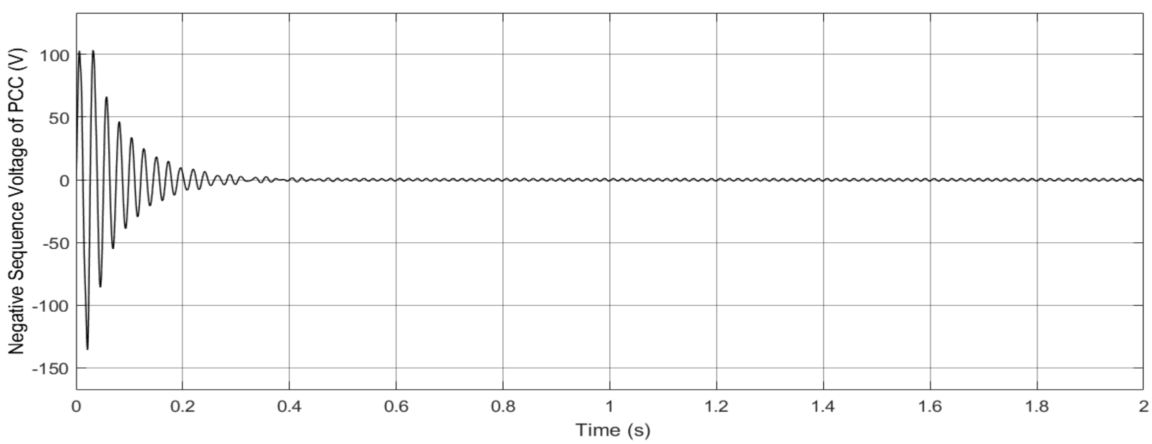

(d)

Fig 3.3. Performance of the Proposed Compensation Method in a Microgrid with Unbalanced Load. (a) Output Voltages of PCC. (b) Output Currents of PCC. (c) VUF at PCC (d) Phase-a Negative Squence Voltage of PCC

To demonstrate the effectiveness of the proposed method in microgrid with unbalanced load, virtual negative impedance and secondary control for unbalanced load compensation are added. After compensation, PCC voltage becomes balance, by making voltages of DGs terminal more unbalanced. When voltage unbalanced is compensated using proposed method, output voltage and current are given in Fig 3.3 (a) to demonstrate unbalanced compensation clearly. This fact can also be observed in Fig 3.3 (c), when VUF of PCC terminal follows reference value (%0.5) from %4.5 and VUF of DGs terminal increased. As seen in Fig 3.3 (d), single phase of negative sequence of fundamental voltage at PCC, compared to the simulated performance in Fig 3.2 (d), PCC negative sequence of fundamental voltage reduced after compensation.

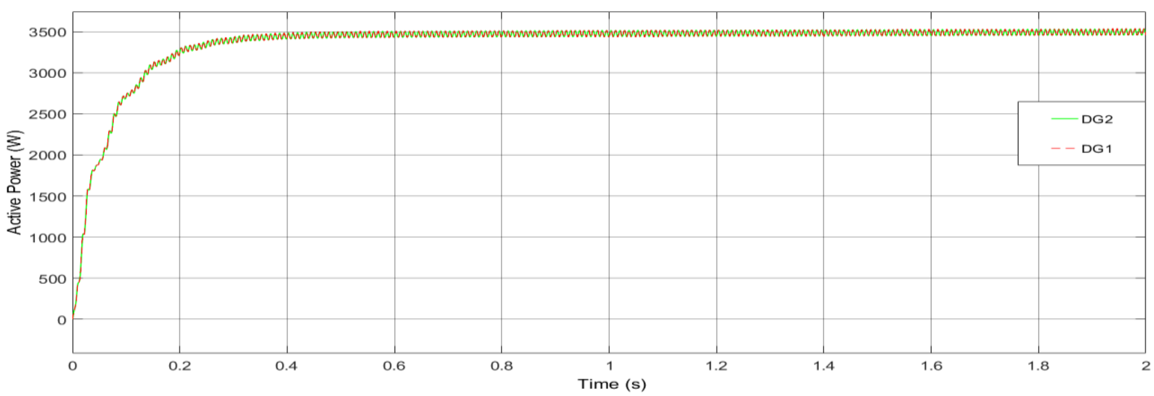

(a)

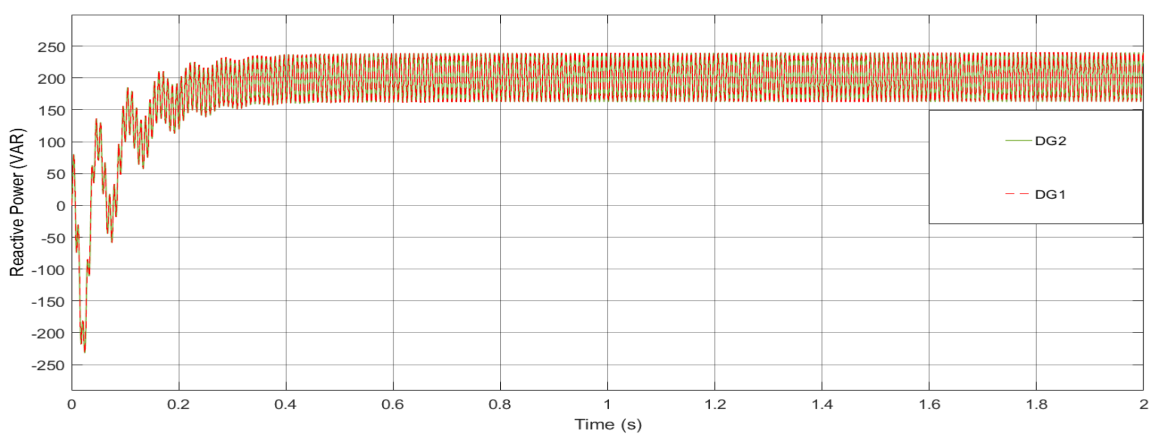

(b)

Fig 3.4. Power Sharing Performance after the Proposed Compensation Method under Unbalanced Load between DGs. (a) Fundamental Positive Active Power. (b) Fundamental Positive Reactive Power

Moreover it can be seen in Fig 3.4 that fundamental positive active and reactive powers between DGs are shared equally. It should be noted that the frequency provided by droop control is the same thus sharing of active power between DGs are exactly equal.

3.2. Results under Nonlinear Load for Step 2

Before activating nonlinear compensation method, droop control and virtual positive impedance in microgrid with nonlinear load are implemented and switch1 is open mode and switch2 is closed state to test harmonic distortion. Fig 3.5 shows the performance of the microgrid when control of VVHI and secondary control for nonlinear load compensation are not performed. Due to nonlinear load, output voltage and current at PCC are distorted noticeably and includes high main harmonic distortion which areHD^{3+},HD^{5-}, HD^{7+}, HD^{11-}andHD^{13+}. Fig 3.5 (c) demonstrates that harmonic distortion(HD) for main selected harmonic sequences which are positive sequence of 3th harmonic, negative sequence of 5th harmonic, positive sequence of 7th harmonic, negative sequence of 11th harmonic and positive sequence of 13th harmonic are high. Furthermore, presence of high at PCC can be observed in Fig 3.5(d).

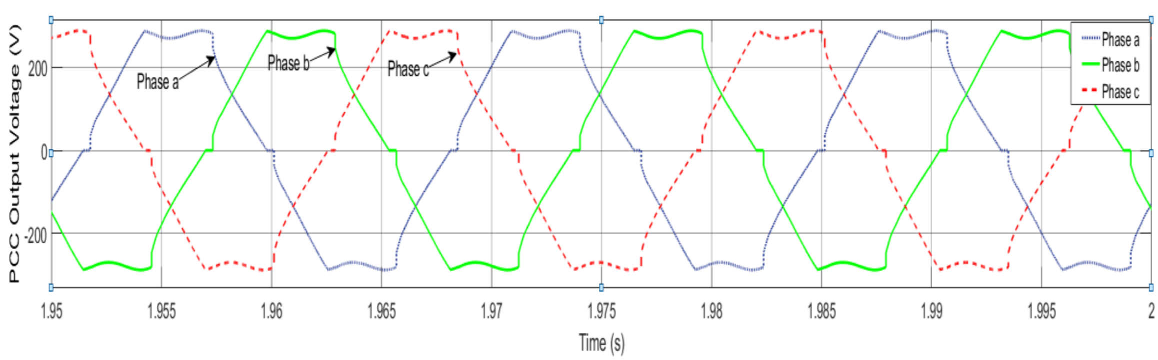

(a) Output Voltages of PCC.

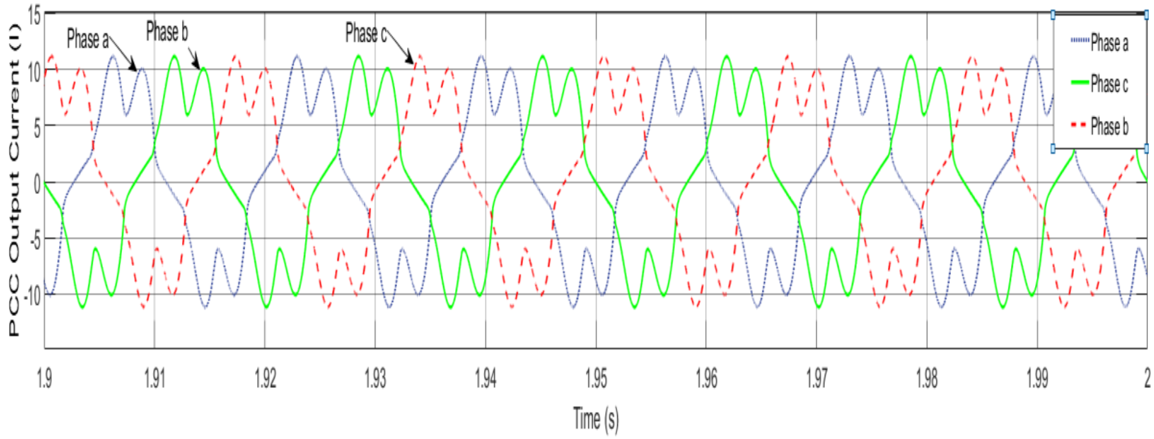

(c) Output Currents of PCC

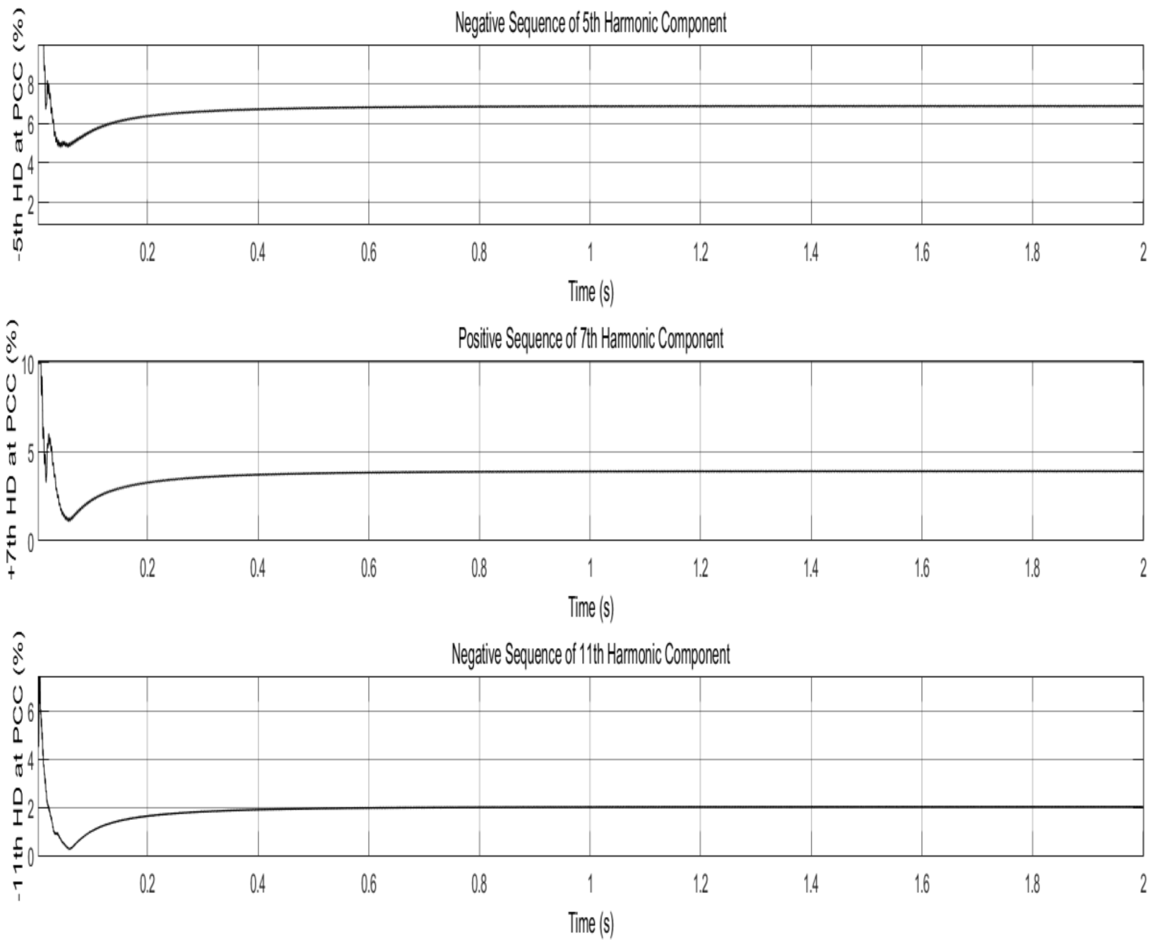

(c) HD for Main Harmonic Sequence at PCC.

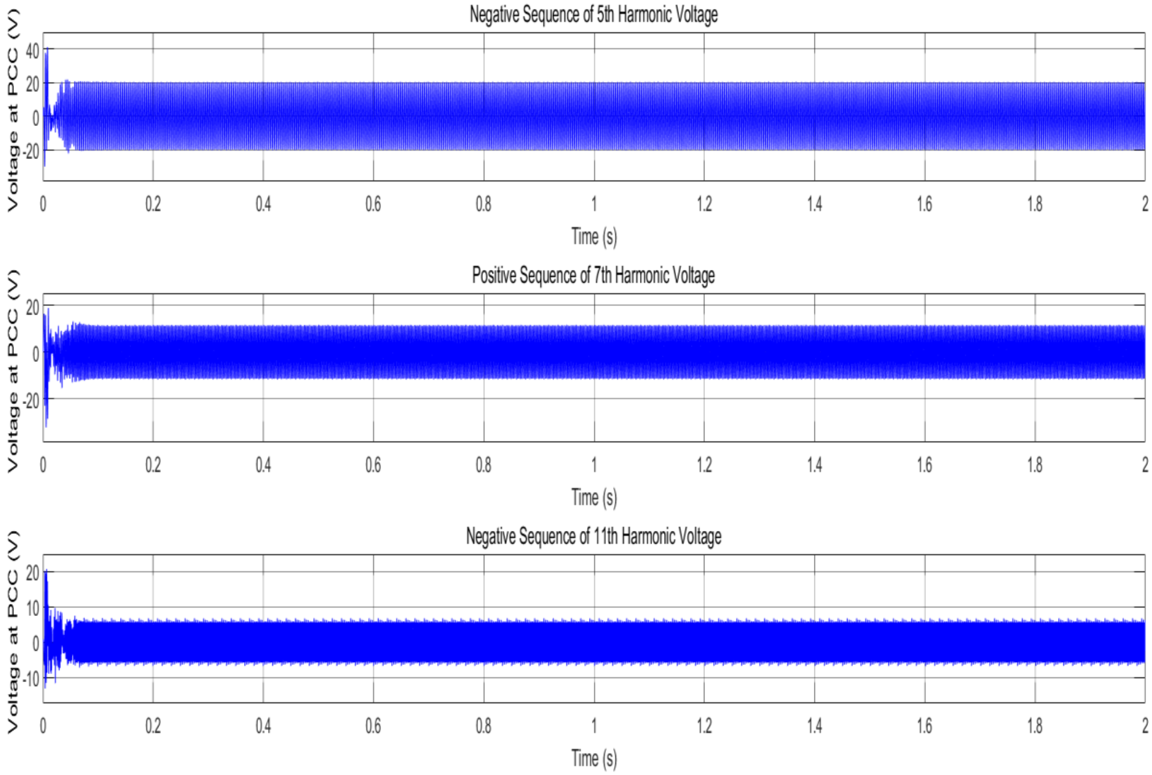

(d)

Fig. 3.5. Performance of the Conventional Droop Control in a Microgrid with Nonlinear Load. (a) Output Voltages of PCC. (b) Output Currents of PCC (c) HD for Main Harmonic Sequence at PCC (d) Voltages of Selected Main Harmonic Sequences at PCC

Virtual harmonic impedance and secondary control for main harmonic compensation are activated. When harmonic distortion is compensated by using the proposed method, PCC voltage quality is significantly enhanced as seen in Fig 3.6. To demonstrate this fact, in Fig 3.6, main harmonic distortion indices (HD^{3+},HD^{5-}, HD^{7+}, HD^{11-}andHD^{13+}) reduce to reference value of harmonic distortion indices (%0.5) to improve voltage quality. It should be noted that harmonic distortion of PCC voltage reduce by increasing harmonic distortion of DGs terminal. The harmonic power also shared equally by sharing PCC output current equally in Fig 3.6 (b) Furthermore, proper sharing of fundamental positive active and reactive powers between DGs is achieved in Fig 3.7 so frequency of microgrid also similar. It can be shown in Fig 3.2.6(d), single phase of selected main harmonic sequences voltage at PCC, decreased after nonlinear proposed compensation compared to the simulated performance in Fig 3.5.

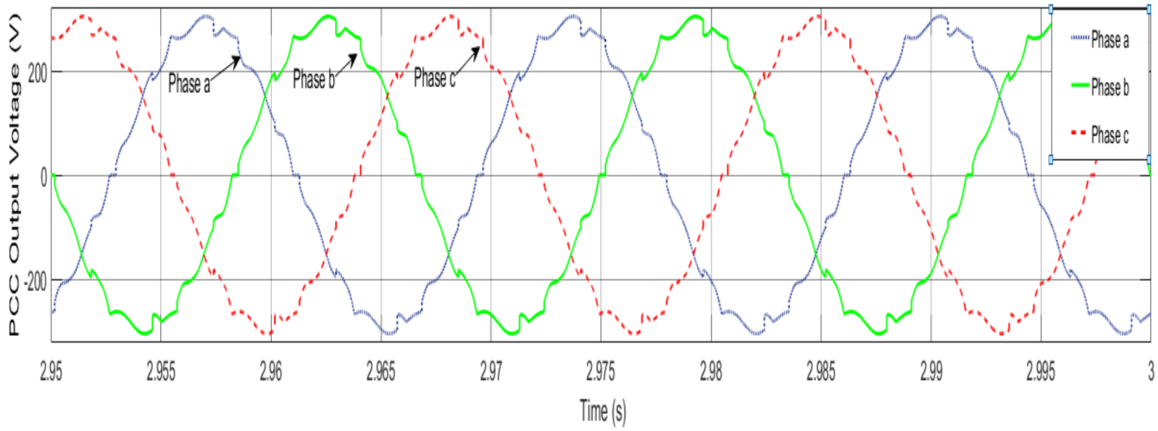

(a) Output Voltages PCC.

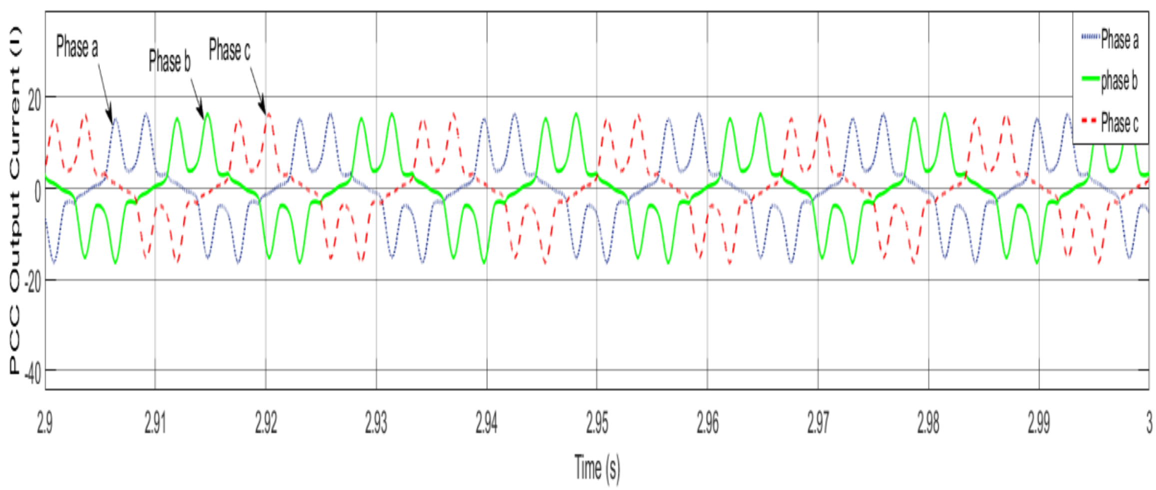

(b) Output Currents of PCC.

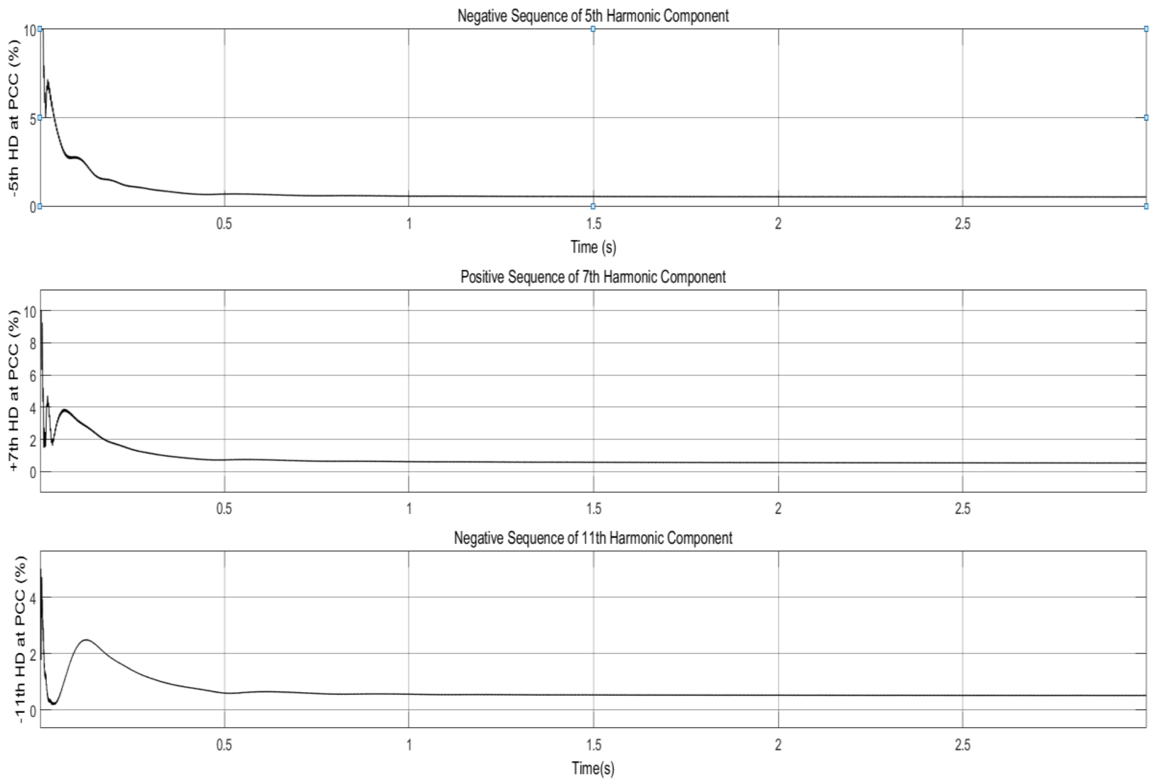

(c)

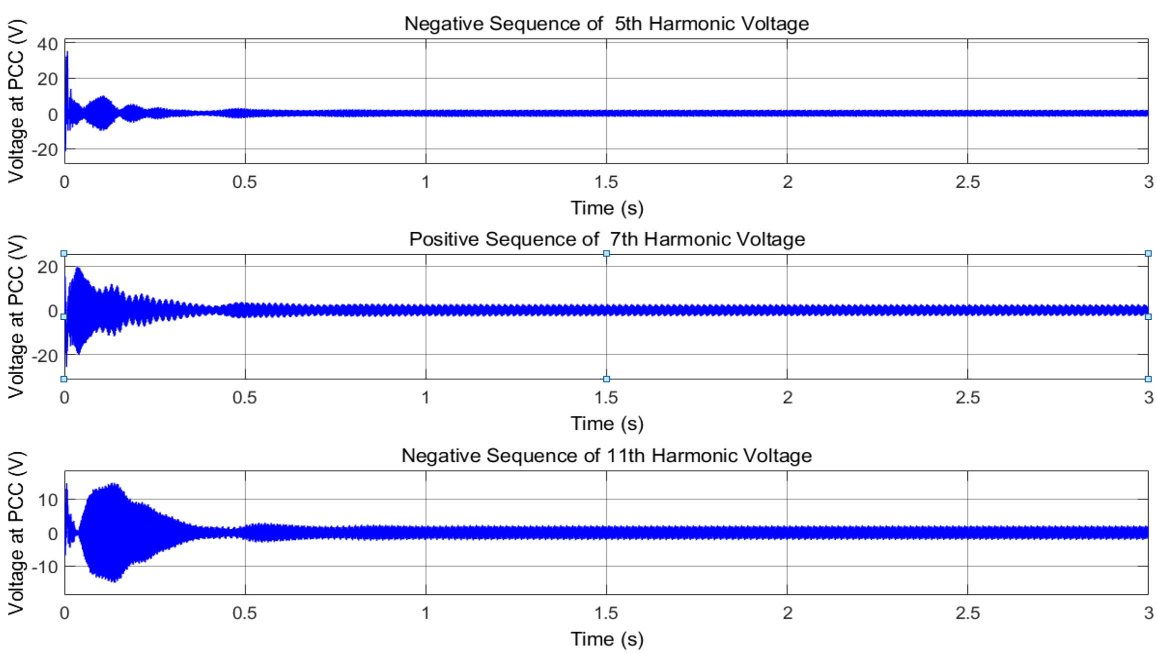

(d)

Fig 3.6. Performance of the Proposed Method in a Microgrid with Nonlinear Load. (a) Output Voltages PCC. (b) Output Currents of PCC. (c) HD for Main Harmonic Sequence at PCC (d) Phase-a Negative Squence Voltage of PCC.

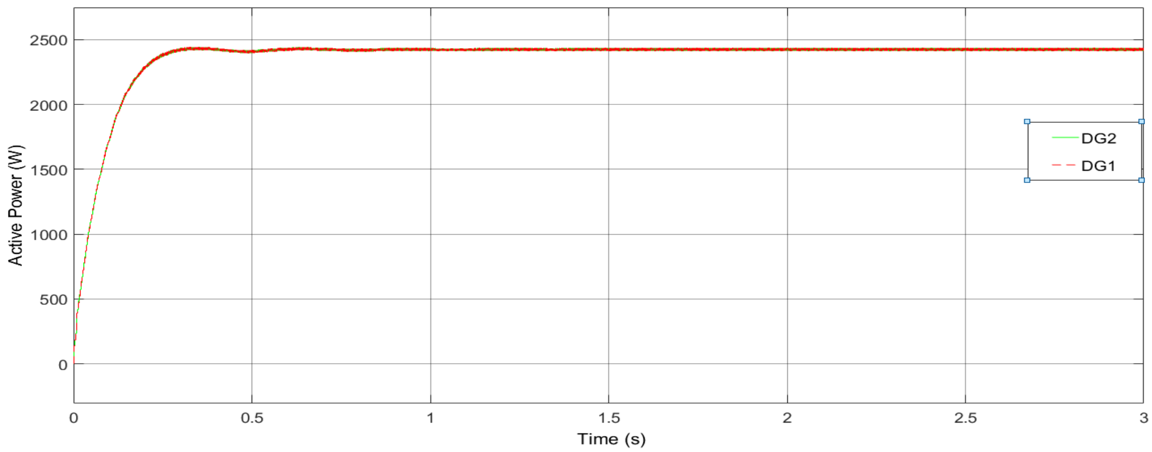

(a)

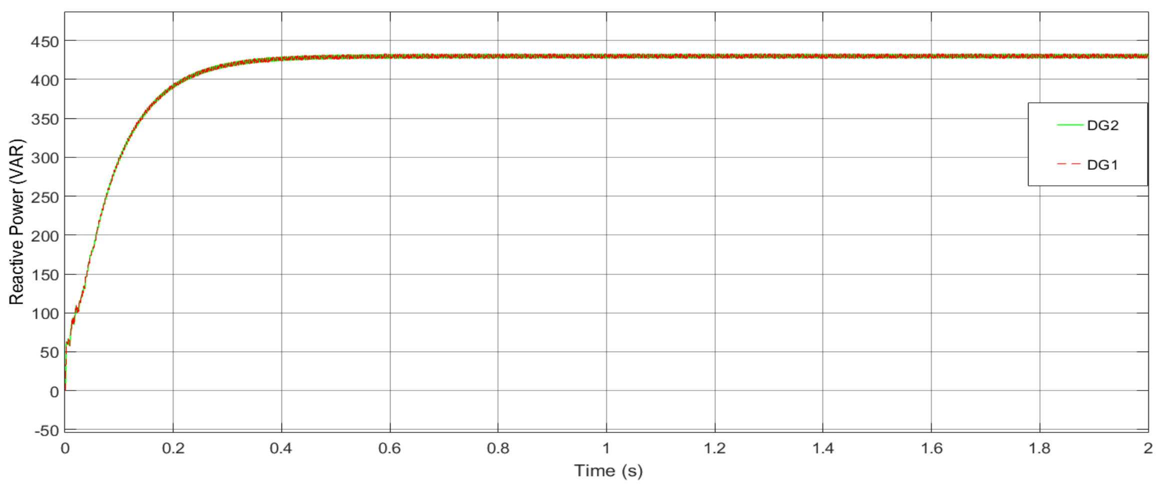

(b)

Fig 3.7. Power Sharing Performance before Compensation Method under Nonlinear Load between DGs. (a) Fundamental Positive Active Power. (b) Fundamental Positive Reactive Power

3.3. Results under Unbalanced Load plus Nonlinear Load for Step 3

Switch1 and switch2 are in the closed state, before activating proposed method. Load sharing of performance using droop control and virtual positive impedance in microgrid with unbalanced load plus nonlinear load connected to the PCC is given in Fig 3.8 (a). As seen, PCC out voltage and currents are unbalanced and distorted highly. To support this fact in the conventional method, high value of voltage unbalanced factor and harmonic distortion indices and existence of high voltage of negative and selected main harmonic sequences at PCC are depicted in Fig 3.8(c) and Fig 3.8 (d) respectively.

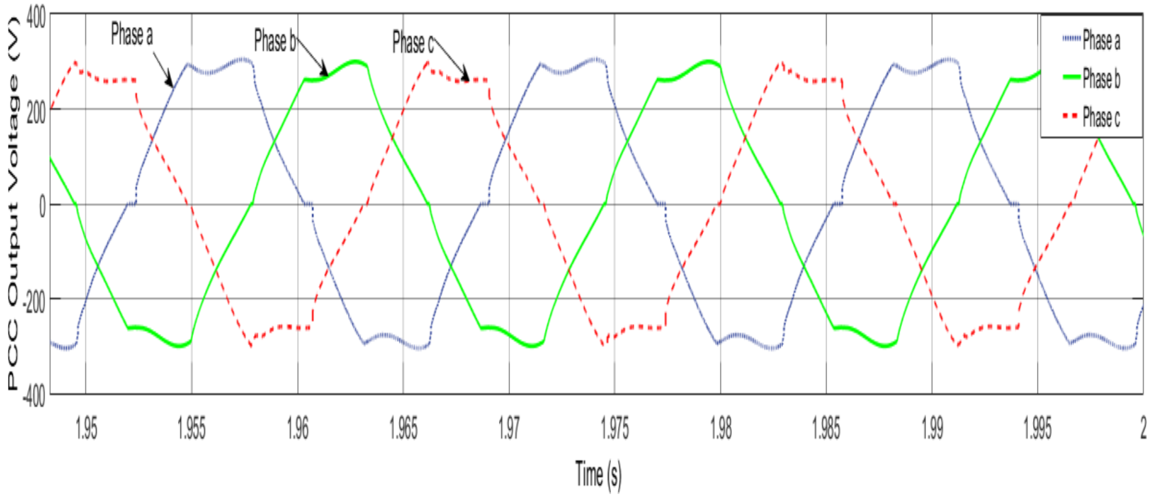

(a) Output Voltages of PCC.

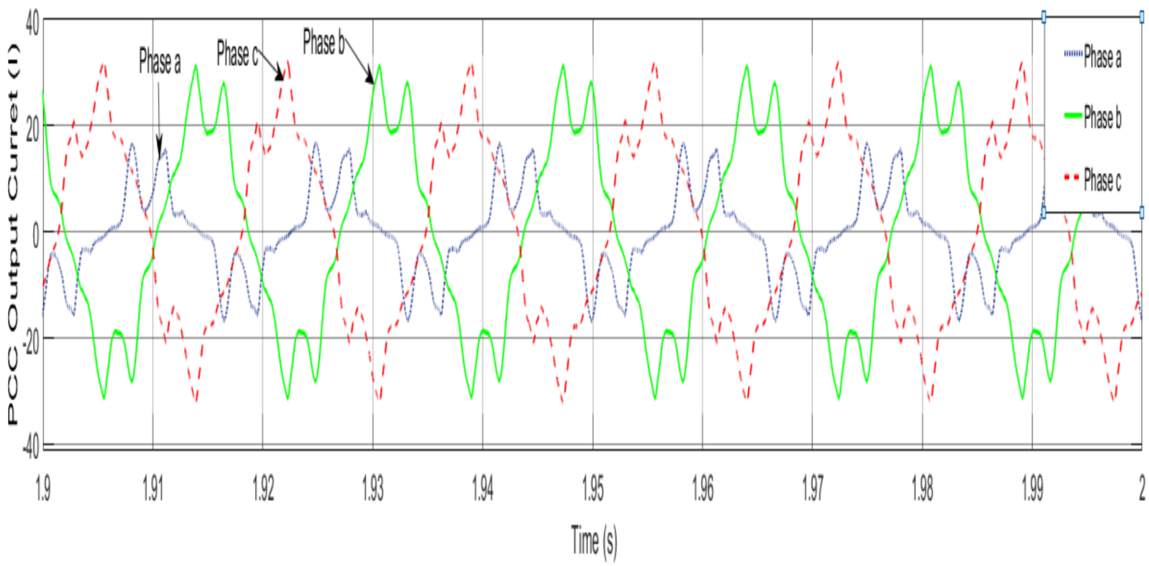

(b) Output Currents of PCC.

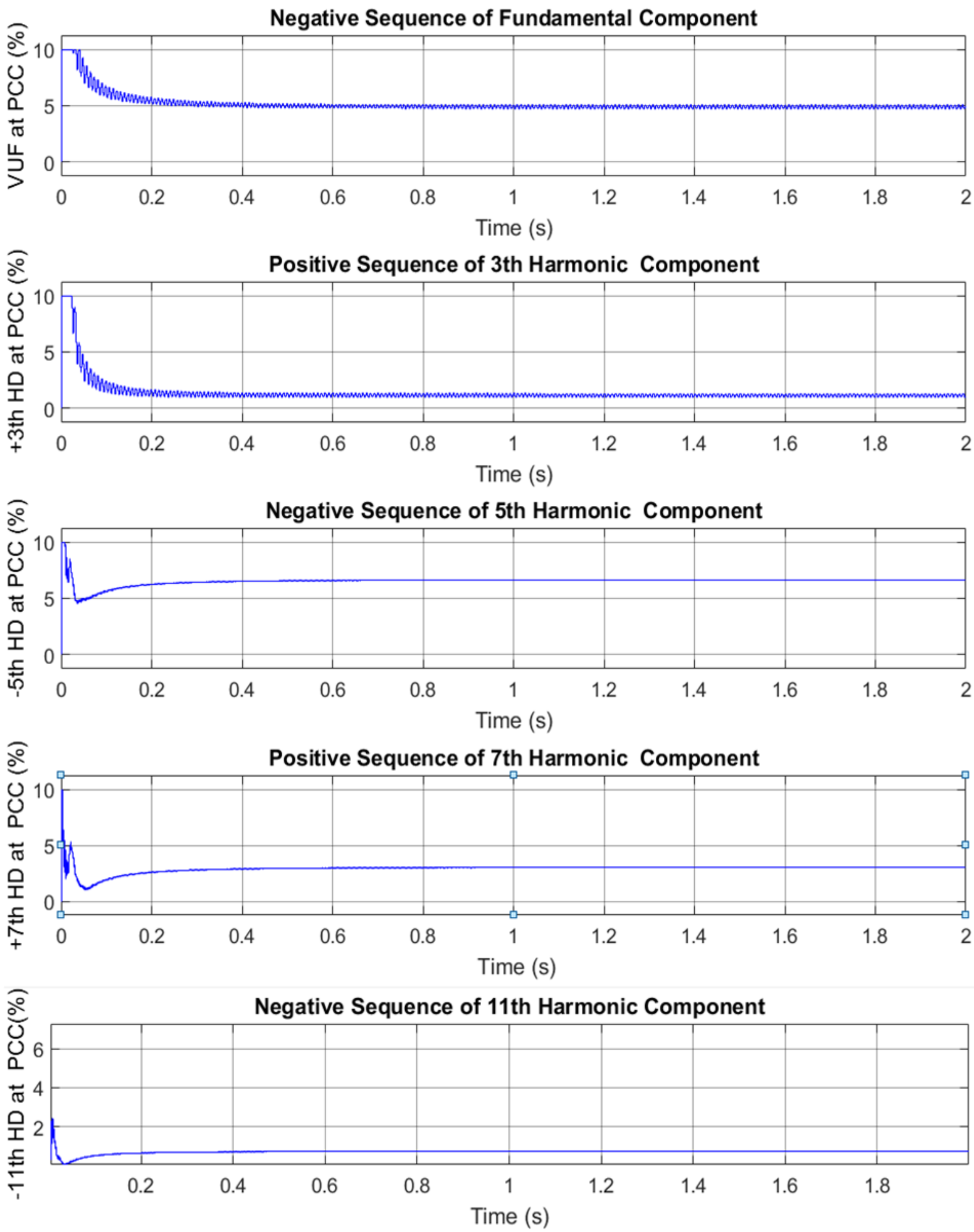

(b) HD for Main Harmonic Sequence at PCC.

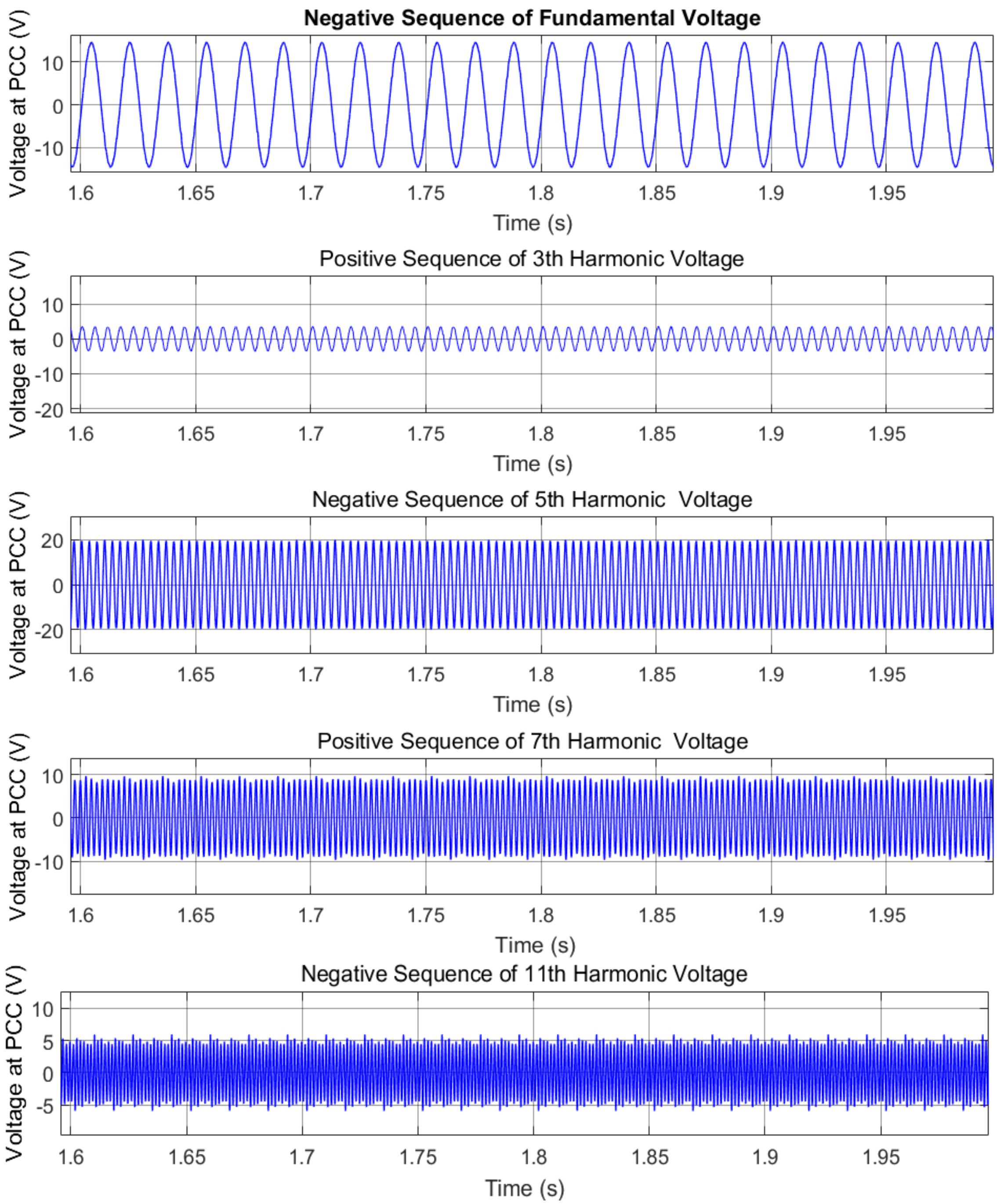

(d)

Figure 3.8 Performance of the Conventional Compensation Method in a Microgrid with Unbalanced plus Nonlinear Load. (a) Output Voltages of PCC. (b) Output Currents of PCC. (c) HD for Main Harmonic Sequence at PCC. (d) Phase-a Negative Squence Voltage of PCC and Voltages of Selected Main Harmonic Sequences at PCC

Virtual negative impedance at fundamental frequency, virtual variable harmonics impedance and secondary control for unbalanced and nonlinear load compensation are adopted. After activation of proposed compensation method, voltage and current qualities of PCC are improved effectively shown in Fig.3.9 (a) and Fig.3.9 (b) respectively compared to the simulated performance in Fig.3.8 (a) and Fig.3.8 (b) Reduction of voltage unbalanced factor and harmonic distortion indices values as seen in Fig.3.9 (c) also verifies improving of PCC voltage quality. Remember that increasing of virtual resistances value for fundamental negative sequence and harmonic components reduces oscillation and help the reduction of UF and HD. To further verify the effectiveness of enhancing PCC voltage, low value of negative and selected main harmonic sequences voltages at PCC can be depicted in Fig 3.9 (d) also.

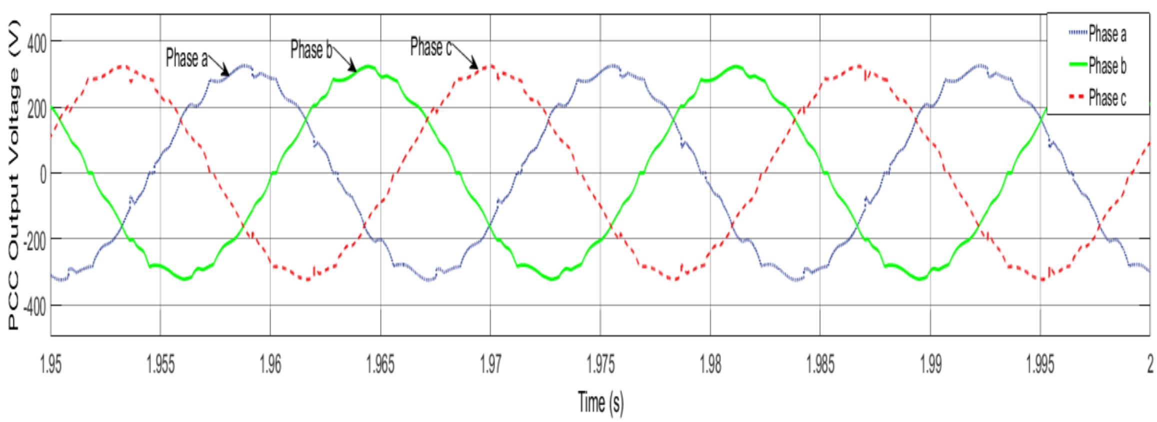

(a) Output Voltages PCC

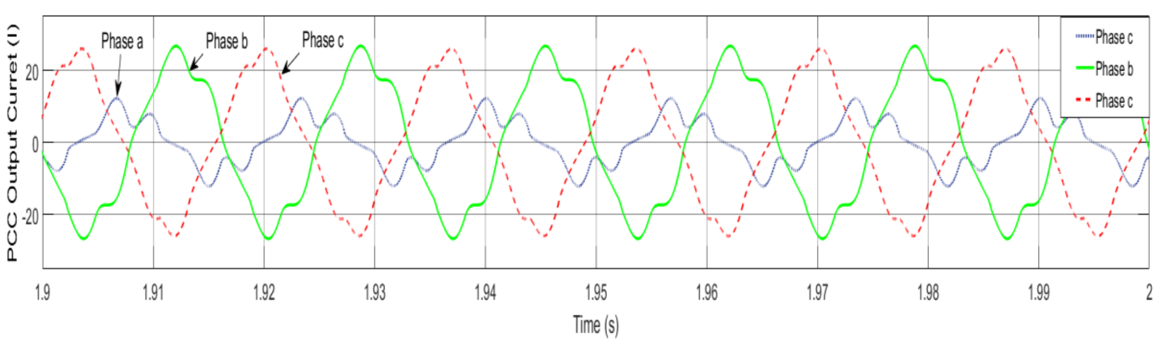

(b) Output Currents of PCC.

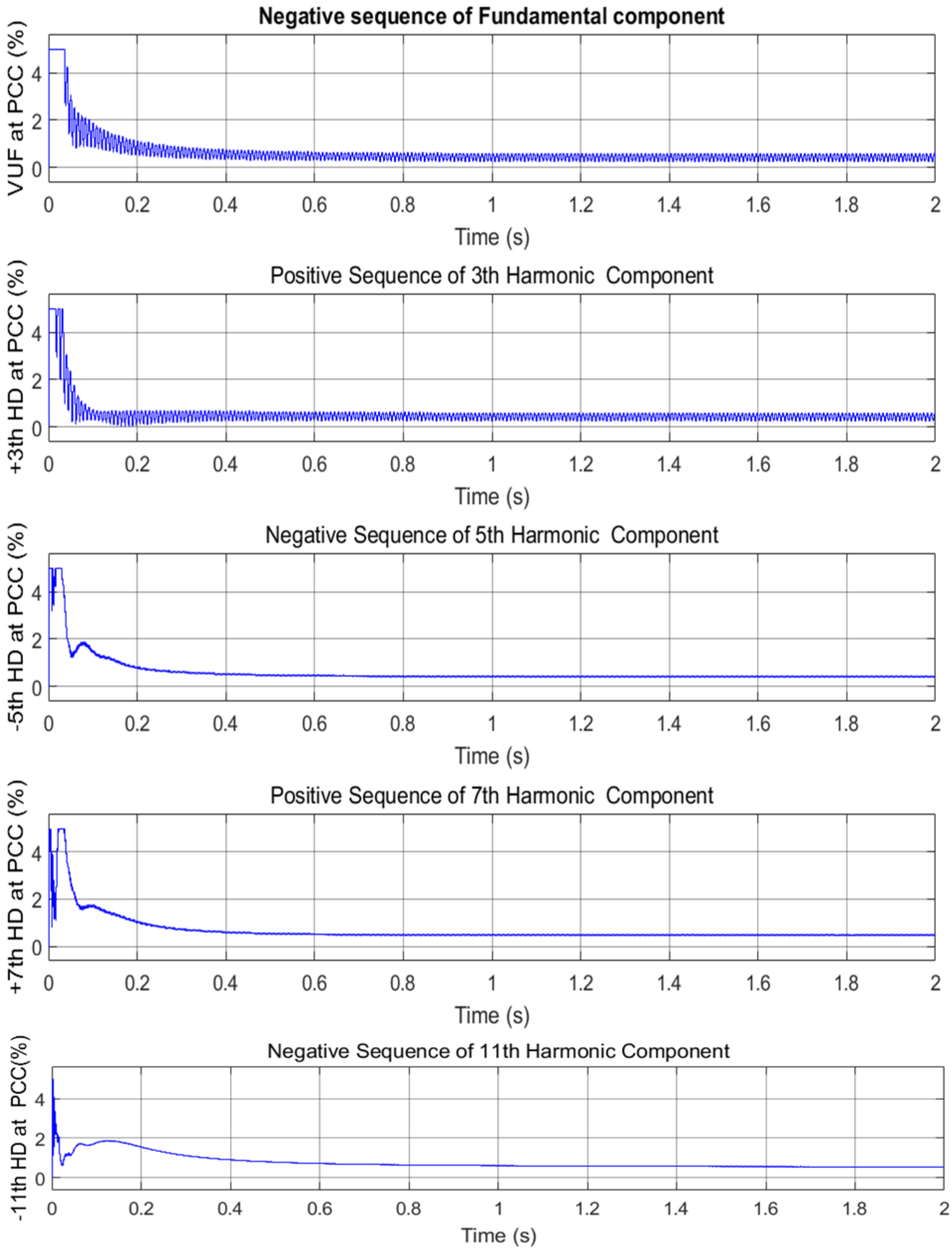

(c) VUF and HD for Main Harmonic Sequence at PCC

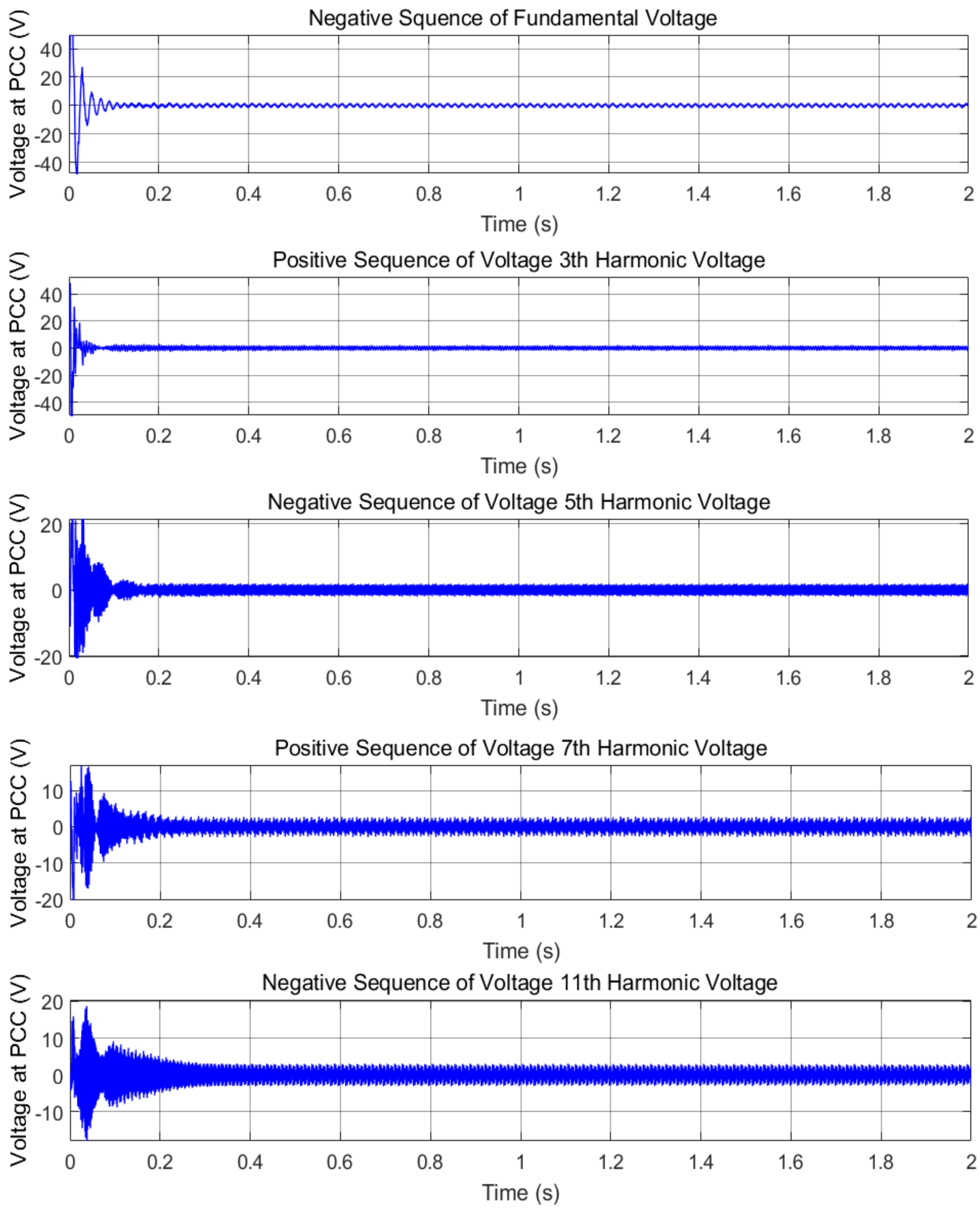

(d)

Fig 3.9. Performance of the Proposed Compensation method in a Microgrid with Unbalanced plus Nonlinear Load. (a) Output Voltages PCC. (b) Output Currents of PCC. (c) VUF and HD for Main Harmonic Sequence at PCC (d) Phase-a Negative and Selected main Harmonic Sequences Voltages at PCC.

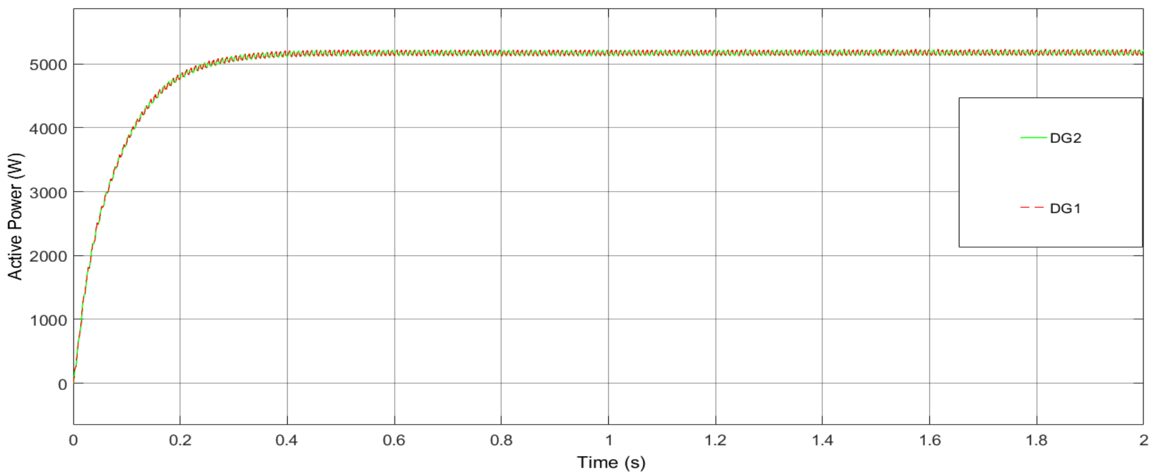

(a)

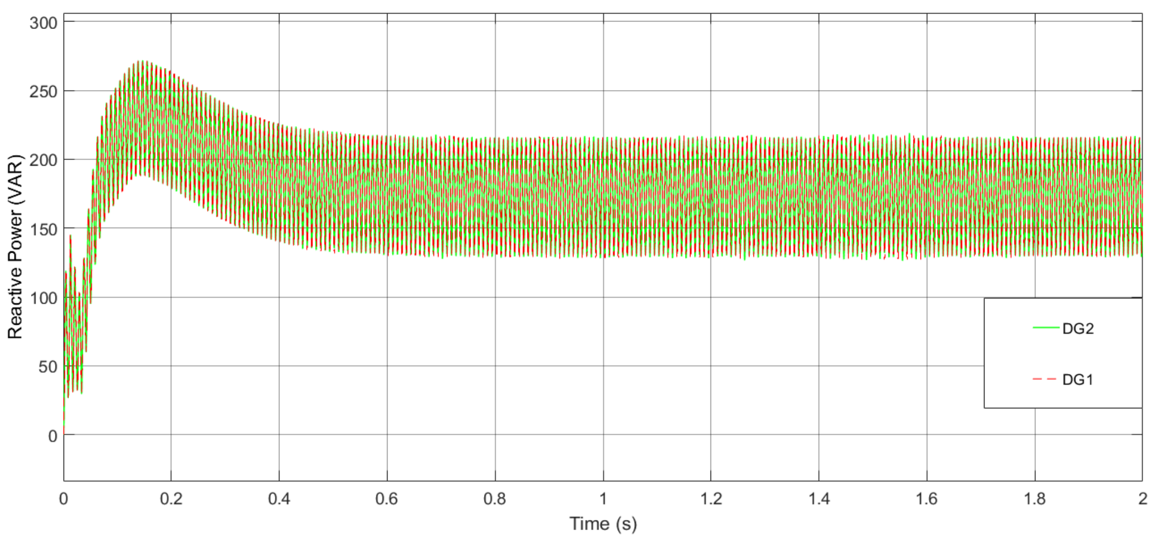

(b)

Fig 3.10. Power Sharing Performance after the Proposed Compensation Method under Unbalanced Load plus Nonlinear Load between DGs. (a) Fundamental Positive Active Power. (b) Fundamental Positive Reactive Power

Under the unbalanced and nonlinear load conditions, fundamental positive active and reactive powers sharing performance are presented as observed in Fig.3.10. It should be noted that power sharing properly between DGs demonstrates the effectiveness of the droop controllers. As aforementioned, the voltage Total harmonic distortion (THD) for sensitive loads should be kept under 5%. Fig 3.11 demonstrates that THD reduced from

9.31% to 4.13% which is less than 5% and it is acceptable result finally to supply in two parallel connected DG units with unbalanced load plus nonlinear load.

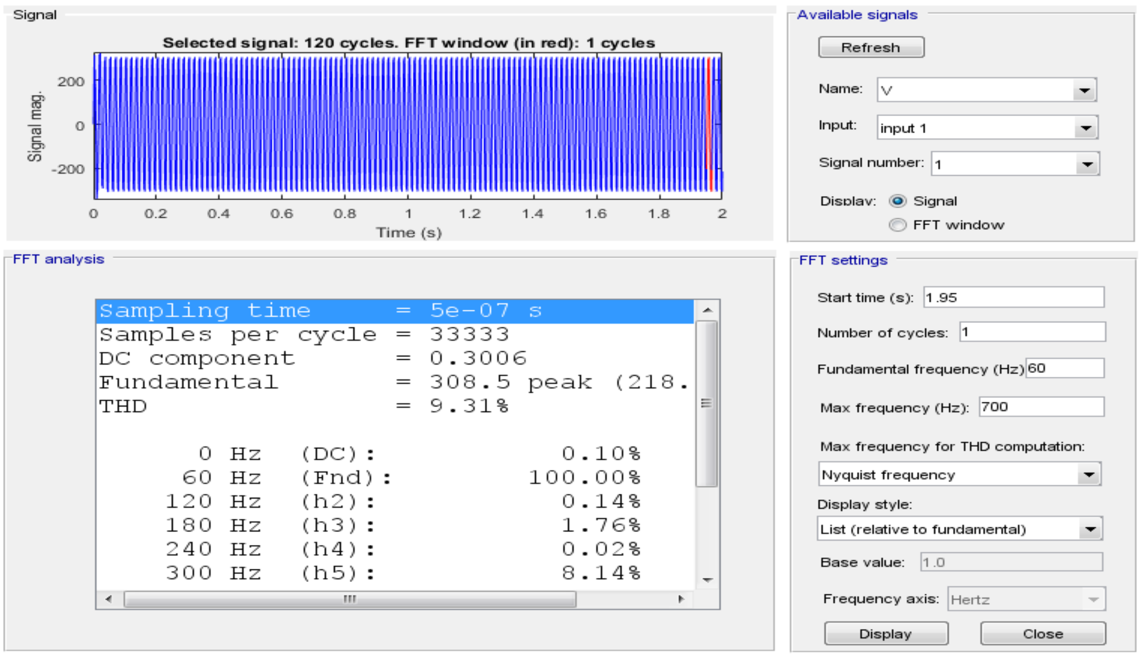

(a)

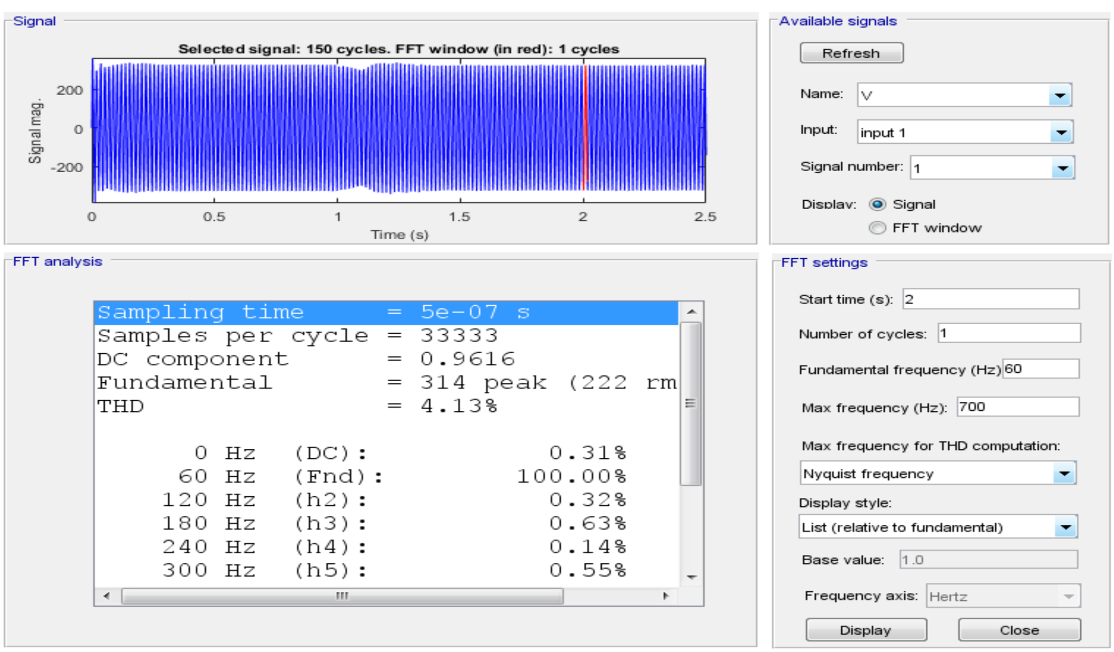

(b)

Fig.3.11 THD of PCC Voltage through FFT under Unbalanced load plus Nonlinear Load (a) Before the Compensation Method. (b) After the Compensation Mehtod.

3.4 Step Load Changing

The performance of step load applied to two parallel DG units is illustrated in Fig 3.12 under unbalanced load plus nonlinear load when a 10 ohm three phase resistive load is suddenly applied at 1 s. it can be seen that adding of the resistive load increases fundamental positive active and reactive power from 5200 W and 180 VAR to 6400 W and 525 VAR at 2 second. On the other hand, applying step load drops microgrid frequency from 49.9 Hz to 49.8 Hz and small deviation is observed in Fig 3.13.

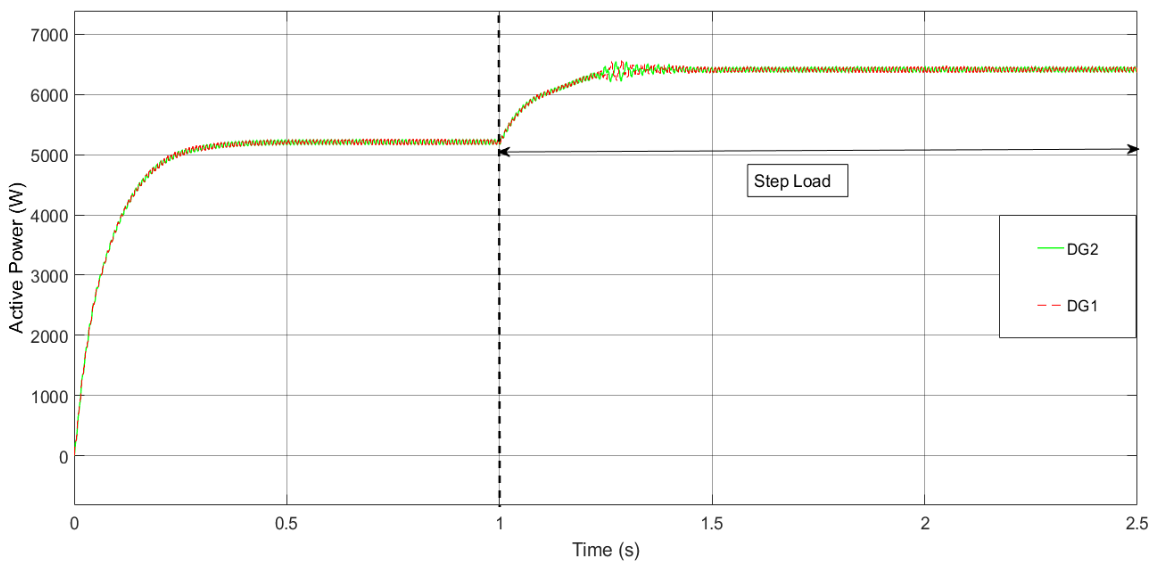

(a)

(a) Fundamental Positive Active Power.

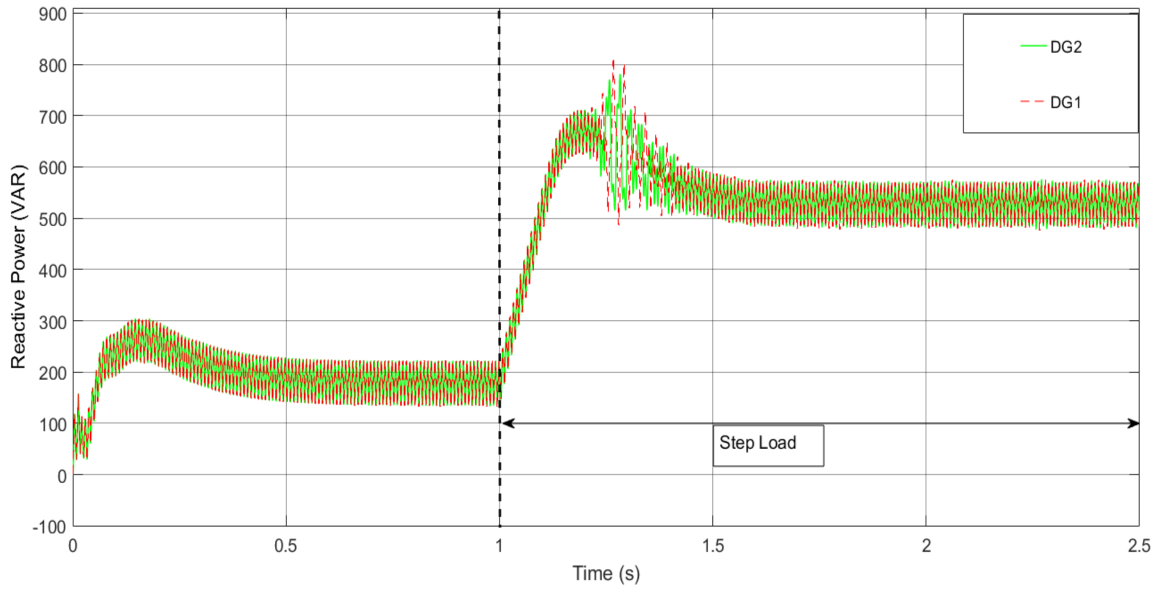

(b)

Fig. 3.12 Step Load Performance with the Proposed Compensation Method under Unbalanced Load plus Nonlinear Load between DGs. (a) Fundamental Positive Active Power. (b) Fundamental Positive Reactive Power

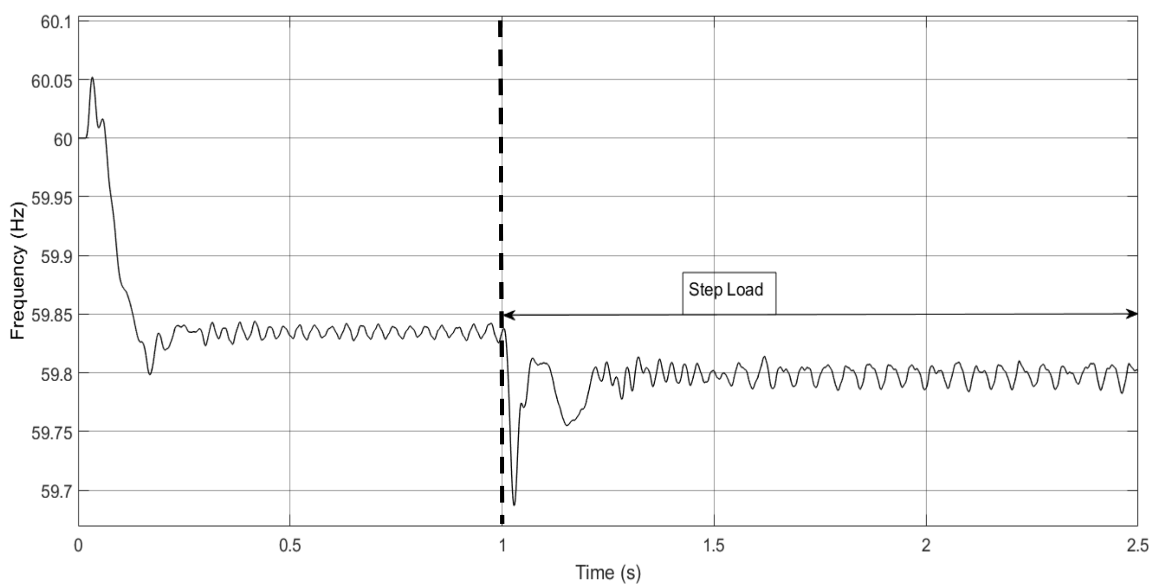

Fig 3.13 Microgrid Frequency by Changing Step Load Performance with the Proposed Compensation Method under Unbalanced Load plus Nonlinear Load.

CHAPTER 4 CONCLUSION

A hierarchical control structure proposes improving power sharing scheme and compensating PCC voltage under unbalanced and harmonic loads in islanding micro grid. The control scheme consists of a primary local controller and secondary controller. Active, reactive, unbalanced and harmonic power sharing inaccurately between DGs and voltage quality problems are significant issues under unbalance and nonlinear loads in parallel inverter. Primary control presents, virtual impedance control and power droop control for sharing fundamental positive active and reactive powers. While droop control is integrated to generate output voltage reference for DGs stage without communication, virtual positive sequence impedance (VPI), virtual negative sequence impedance (VNI) and virtual variable harmonics impedance (VVHI) are presented to improve sharing of unbalanced and harmonic current equally. Negative sequence of fundamental component and positive and negative sequence of voltage main harmonics are compensated in secondary control for PCC voltage quality improvement. In addition, PR controls are used to track capacitor voltage and inductor current. To extract positive and negative sequences of fundamental and harmonic components for inductor current through virtual impedance loop, SOGI is designed. Proper PCC data and signal are sent from secondary control to primary control. Moreover, each DG unit should be controlled to be proportional to its power rating in the islanded mode [10].

The control system design, output impedance and close loop transfer function is discussed in detail. As the next step, simulation on MATLAB to demonstrate the effectiveness of the proposed control scheme are considered in three steps under unbalanced and harmonic conditions. The effectiveness of the proposed control scheme in simulation results is validated that PCC voltage distortion decreased noticeably while active and reactive powers are shared properly after compensation. As a result, Simulation results are verifying that the proposed control is applicable in the two parallel connected inverters application.

CHAPTER 5 FUTURE SCOPE of WORK

While powers sharing proportionally and improving quality of PCC output voltage are achieved under unbalanced and nonlinear loads in the islanding microgrid, the proposed method can be enhanced by making complex and adding proper controls. In the proposed method, there were just two DGs and each DG unit had the same capacity. As a future work, multi DGs can be operated independently and different rating DGs can be used in the islanded mode, then each DG will share power to be proportional to its power rating. Furthermore, each feeder impedance in the DGs had the same inductance value in the method, however sometimes feeder impedance contains resistance and inductance together. Using different feeder impedances with resistance and inductance does not allow reactive power sharing accurately. By modifying droop control and virtual impedance control, reactive power sharing error will reduce. In addition, droop control decreased frequency and magnitude of DG out voltage to fundamental positive active and reactive powers. The frequency and magnitude of inverter will be restored and increased to nominal values by enhancing secondary control. Another work will be to improve output voltage quality of DG units. To compensate PCC output voltage, secondary control sent compensation reference signal to primary control by distorting DG output voltage. The active power filter will be proposed to reduce harmonic distortion of DGs. As a result, as the next steps, using more than two and different rating DG units, different feeder impedances, fixing frequency and magnitude of output inverter and improving output voltage quality of DG units will be worked under unbalanced and nonlinear loads in the islanding microgrid.

REFERENCES

[1] H. Farhangi, “The Path of the Smart Grid,” IEEE power & energy Mag., vol.8 no.1, pp. 18-28 Jan. /Feb. 2010.

[2] X. Fang, S. Misra, G. Xue, and D Yang, “Smart Grid – The New and Improved Power Grid: A Surve” IEEE com. surveys & tutorials, vol. 14, no. 4, pp. 994-980, fourth quarter 2012.

[3] S. M. Amin and B. F. Wollenberg, “Toward a smart grid,” IEEE Power Energy Mag., vol. 3, no. 5, pp. 34–41, Sep./Oct. 2005.

[4] V. C. Gungor, B. Lu, and G. P. Hancke, “Opportunities and challenges of wireless sensor networks in smart grid,” IEEE Trans. Ind. Electron., vol. 57, no. 10, pp. 3557–3564, Oct. 2010.

[5] V. C. Gungor, D. Sahin, T. Kocak, S. Ergut, C. Buccella, Carlo Cecati and G. P. Hancke, “Smart Grid Technologies: Communication Technologies and Standards,” IEEE Trans. Ind. informatics., vol. 7, no. 4, pp. 529–538, Nov. 2011.

[6] M. Savaghebi, A. Jalilian, J. C. Vasquez and J. M. Guerrero, “Secondary Control Scheme for Voltage Unbalance Compensation in an Islanded Droop-Controlled Microgrid,” in IEEE Transactions on Smart Grid, vol. 3, no. 2, pp. 797-807, June 2012.

[7] W. Cao, H. Su W. China, J. Cao, J. Sun, D. Yang “Improved Droop Control Method in Microgrid and Its Small Signal Stability Analysis,” 3rd International Conference on Renewable Energy Research and Applications, pp. 197-202, 19-22 Oct 2014.

[8] J. He, Y. W. Li and F. Blaabjerg, “An Enhanced Islanding Microgrid Reactive Power, Imbalance Power, and Harmonic Power Sharing Scheme,” in *IEEE Transactions on Power Electronics*, vol. 30, no. 6, pp. 3389-3401, June 2015.

[9] M. Savaghebi, A. Jalilian, J. C. Vasquez and J. M. Guerrero, "Secondary Control for Voltage Quality Enhancement in Microgrids," in *IEEE Transactions on Smart Grid*, vol. 3, no. 4, pp. 1893-1902, Dec. 2012.

[10] Y. Han, P. Shen, X. Zhao and J. M. Guerrero, "An Enhanced Power Sharing Scheme for Voltage Unbalance and Harmonics Compensation in an Islanded AC Micro grid," in *IEEE Transactions on Energy Conversion*, vol. 31, no. 3, pp. 1037-1050, Sept. 2016.

[11] Q. Liu, Y. Tao, X. Liu, Y. Deng and X. He, "Voltage unbalance and harmonics compensation for islanded microgrid inverters," in *IET Power Electronics*, vol. 7, no. 5, pp. 1055-1063, May 2014.

[12] S. Khongkhachat and S. Khomfoi, "Droop control strategy of AC micro grid in islanding mode," *Electrical Machines and Systems (ICEMS), 2015 18th International Conference on*, Pattaya, 2015, pp. 2093-2098.

[13] S. Bruno, S. Lamonaca, G. Rotondo, U. Stecchi, and M. L. Scala, “Unbalanced three-phase optimal power flow for smart grids,” *IEEE Trans. Ind. Electron*., vol. 58, no. 10, pp. 4504–4513, Oct. 2011.

[14] J. He, Y. W. Li, and M. S. Munir, “A flexible harmonic control approach through voltage controlled DG-grid interfacing converters,” *IEEE Trans. Ind. Electron*., vol. 59, no. 1, pp. 444–455, Jan. 2012.

[15] T. L. Lee and P. T. Cheng, “Design of a new cooperative harmonic filtering strategy for distributed generation interface converters in an islanding network,” *IEEE Trans. Power Electron.*, vol. 22, no. 5, pp. 1919–1927, Sep. 2007.

[16] A. V. Jouanne and B. Banerjee, “Assessment of voltage unbalance,” IEEE Trans. Power Del., vol. 16, no. 4, pp. 782–790, Oct. 2001.

[17] A. Chandra, B. Singh, B. N. Singh, and K. Al-Haddad, “An improved control algorithm of shunt active filter for voltage regulation, harmonic elimination, power factor correction, and balancing of nonlinear loads,” IEEE Trans. Power Electron., vol. 15, no. 3, pp. 495–507, May 2000.

[18] M. S. Hamad, M. I. Masoud, and B. W. Williams, “Medium-voltage 12- pulse converter: output voltage harmonic compensation using a series APF,” IEEE Trans. Ind. Electron., vol. 61, no. 1, pp. 43–52, Jan. 2014.

[19] IEEE Standard 519-1992, IEEE recommended practices and requirements for harmonic control in electrical power systems, 1992.

[20] M. Savaghebi, J. C. Vasquez, A. Jalilian, J. M. Guerrero, and T. L. Lee, “Selective compensation of voltage harmonics in grid-connected microgrids,” *Math. Comput. Simul.*, vol. 9, pp. 211–228, May. 2013.

[21] M. Savaghebi, A. Jalilian, J. C. Vasquez and J. M. Guerrero, "Autonomous Voltage Unbalance Compensation in an Islanded Droop-Controlled Microgrid," in *IEEE Transactions on Industrial Electronics*, vol. 60, no. 4, pp. 1390-1402, April 2013.

[22] E. A. A. Coelho, P. Cabaleiro, and P. F. Donoso, Small signal stability

for single phase inverter connected to stiff AC system, in *Proc. IEEEIAS*

99 Annu. Meeting, 1999, pp. 21802187.

[23] J. M. Guerrero, L. G. de Vicuna, J. Matas, M. Castilla and J. Miret, "A wireless controller to enhance dynamic performance of parallel inverters in distributed generation systems," in *IEEE Transactions on Power Electronics*, vol. 19, no. 5, pp. 1205-1213, Sept. 2004.

[24] M. Savaghebi, J. M. Guerrero, A. Jalilian and J. C. Vasquez, "Experimental evaluation of voltage unbalance compensation in an islanded microgrid," *2011 IEEE International Symposium on Industrial Electronics*, Gdansk, 2011, pp. 1453-1458.

[25] J. M. Guerrero, J. C. Vasquez, J. Matas, L. G. de Vicuna and M. Castilla, "Hierarchical Control of Droop-Controlled AC and DC Microgrids—A General Approach Toward Standardization," in *IEEE Transactions on Industrial Electronics*, vol. 58, no. 1, pp. 158-172, Jan. 2011.

[26] Y. Sun, X. Hou, J. Yang, H. Han, M. Su and J. M. Guerrero, "New Perspectives on Droop Control in AC Microgrid," in *IEEE Transactions on Industrial Electronics*, vol. 64, no. 7, pp. 5741-5745, July 2017.

[28] J. M. Guerrero, J. Matas, L. G. de Vicuna, N. Berbel and J. Sosa, "Wireless-control strategy for parallel operation of distributed generation inverters," *Proceedings of the IEEE International Symposium on Industrial Electronics, 2005. ISIE 2005,* Dubrovnik, Croatia, 2005, pp. 845-850 vol. 2.

[29] Q. Huang and K. Rajashekara, "An inverter-current-feedback based reactive power sharing method for parallel inverters in microgrid," *2016 IEEE Energy Conversion Congress and Exposition (ECCE),* Milwaukee, WI, 2016, pp. 1-7.

[30] P. Rodriguez, A. V. Timbus, R. Teodorescu, M. Liserre and F. Blaabjerg, "Flexible Active Power Control of Distributed Power Generation Systems During Grid Faults," in *IEEE Transactions on Industrial Electronics*, vol. 54, no. 5, pp. 2583-2592, Oct. 2007.

[31] P. Rodriguez, A. Luna, I. Candela, R. Mujal, R. Teodorescu and F. Blaabjerg, "Multiresonant Frequency-Locked Loop for Grid Synchronization of Power Converters Under Distorted Grid Conditions," in *IEEE Transactions on Industrial Electronics*, vol. 58, no. 1, pp. 127-138, Jan. 2011.

[32] C. Bao, X. Ruan, X. Wang, W. Li, D. Pan and K. Weng, "Step-by-Step Controller Design for LCL-Type Grid-Connected Inverter with Capacitor–Current-Feedback Active-Damping," in *IEEE Transactions on Power Electronics*, vol. 29, no. 3, pp. 1239-1253, March 2014.

[33] D. Zammit, C. S. Staines, M. Apap, J. Licari, "Design of PR current control with selective harmonic compensators using Matlab," *Journal of Electrical Systems and Information Technology*, Available online 25 January 2017, ISSN 2314-7172.

[34] X. Wang, J. M. Guerrero, F. Blaabjerg and Z. Chen, "Secondary voltage control for harmonics suppression in islanded microgrids," *2011 IEEE Power and Energy Society General Meeting*, San Diego, CA, 2011, pp. 1-8.

[35] X. Guo, Z. Lu, B. Wang, X. Sun, L. Wang and J. M. Guerrero, "Dynamic Phasors-Based Modeling and Stability Analysis of Droop-Controlled Inverters for Microgrid Applications," in *IEEE Transactions on Smart Grid*, vol. 5, no. 6, pp. 2980-2987, Nov. 2014.

[36] M. Savaghebi, J. C. Vasquez, A. Jalilian, J. M. Guerrero and T. L. Lee, "Selective harmonic virtual impedance for voltage source inverters with LCL filter in

microgrids," *2012 IEEE Energy Conversion Congress and Exposition (ECCE)*, Raleigh, NC, 2012, pp. 1960-1965.

[37] Y. Han, P. Shen, X. Zhao and J. M. Guerrero, "Control Strategies for Islanded Microgrid Using Enhanced Hierarchical Control Structure With Multiple Current-Loop Damping Schemes," in *IEEE Transactions on Smart Grid*, vol. 8, no. 3, pp. 1139-1153, May 2017.

[38] F. Guo and C. Wen, "A distributed voltage unbalance compensation method for islanded microgrid," *2015 IEEE 13th International Conference on Industrial Informatics (INDIN)*, Cambridge, 2015, pp. 1140-1145.

[39] A. Cziker, M. Chindris and A. Miron, "Voltage unbalance mitigation using a distributed generator," *2008 11th International Conference on Optimization of Electrical and Electronic Equipment*, Brasov, 2008, pp. 221-226.

[40] B. Bhutia, M.Ali and N. Tiadi, "Design of three phase PWM voltage source inverter for photovoltaic application," *international journal of innovative research in electrical, electronics, instrumentation and control engineering*, Vol. 2, Issue 4, April 2014.

[41] N. I. Raju, S Islam, A. A Uddin, "Sinusoidal PWM signal generation technique for three phase voltage source inverter with analog circuit & simulation of PWM inverter for standalone load & micro-grid system" *international journal of renewable energy research nazmul islam raju ,* Vol.3, No.3.